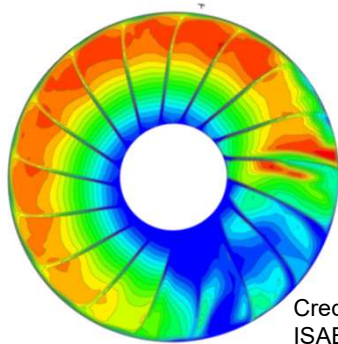


DJINN-ENODISE Conference, Berlin, 22-24 Nov 2023

EXPERIMENTAL INVESTIGATION OF THE INFLUENCE OF BOUNDARY LAYER INGESTION ON TURBO-FAN NOISE GENERATION

Ulf Tapken¹, Robert Meyer¹, Lukas Klähn¹, Maximilian Behn¹, Timea Lengyel-Kampmann²
DLR Institute of Propulsion Technology, Engine Acoustics¹, Fan and Compressor²

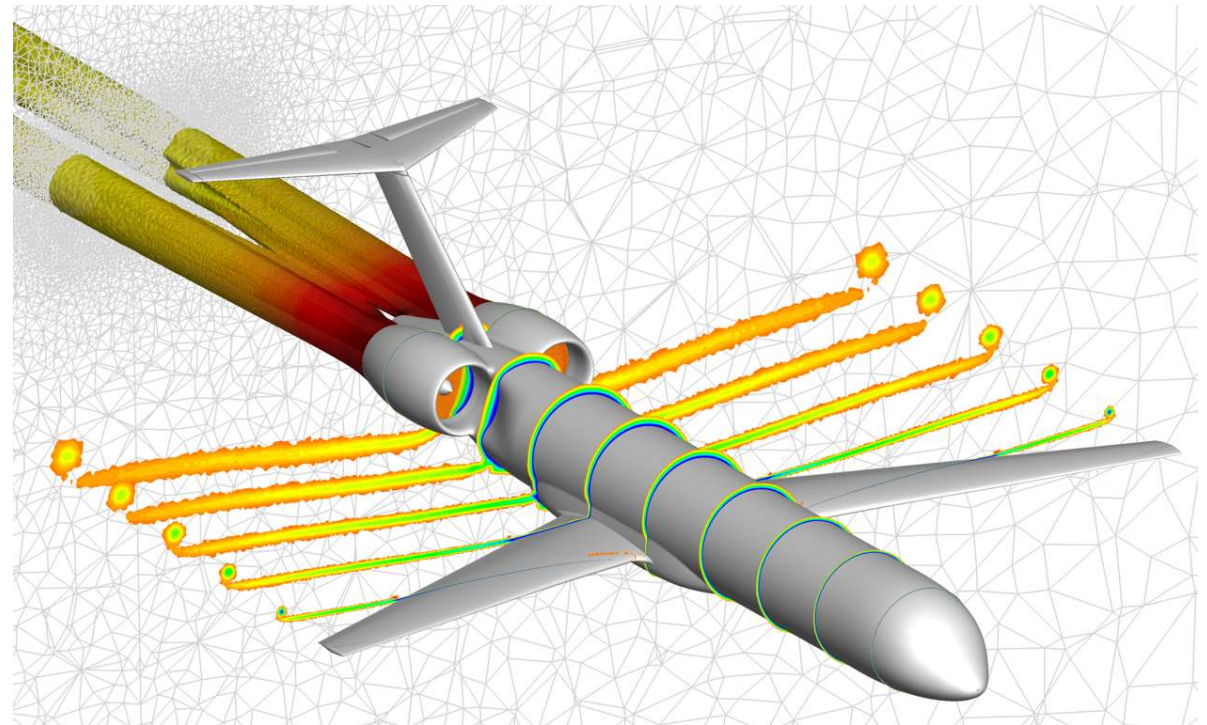
Impact of boundary layer ingestion on aeroengine fans



Credits: Schönweitz et al,
ISABE-2015-22008

Fan blade experiences varying incident flow, leading to e.g.

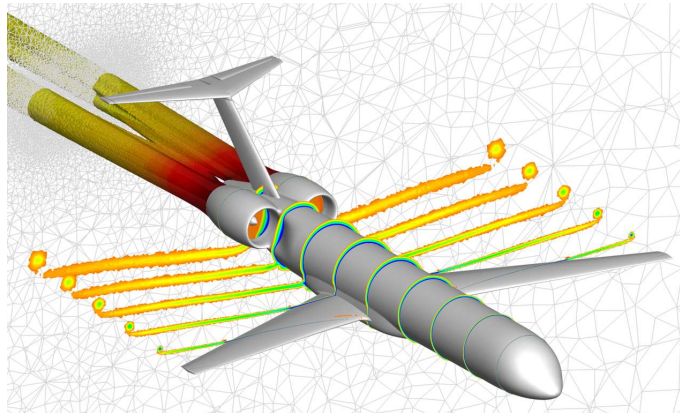
- reduced fan efficiency
- blade vibrations of low orders
- transient structural loads
- additional noise sources



DLR project AGATA^{3S} (2017-2022)



Modelling of aircraft and engine



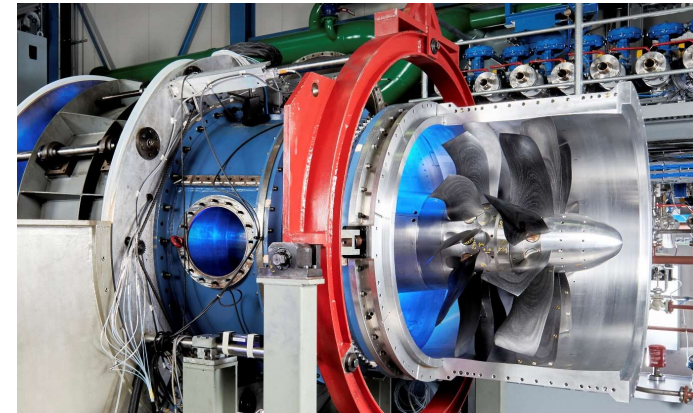
test cases



findings



Experiments under realistic conditions



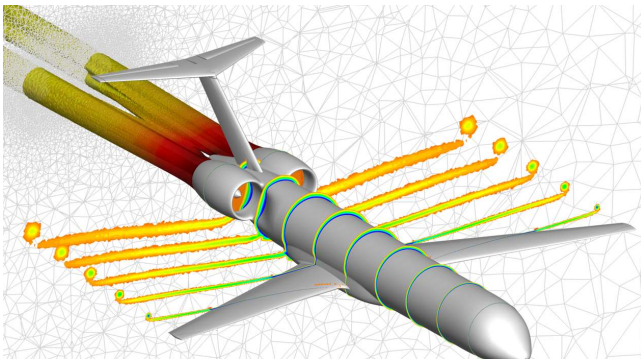
- **Institute of Propulsion Technology**
Engine Acoustics (Berlin), Fan and Compressor (Cologne),
Engine (Cologne), Engine Measurement Systems (Cologne)
- **Institute of Aeroelasticity**
Aeroelasticity of Turbomachinery (Göttingen)

- **Institute of Structures and Design**
Design and Manufacture Technologies (Stuttgart)
- **Institute of Aerodynamics and Flow Technology**
Transport Aircraft (Braunschweig), Technical Acoustics
(Braunschweig)

Derivation of representative BLI test cases

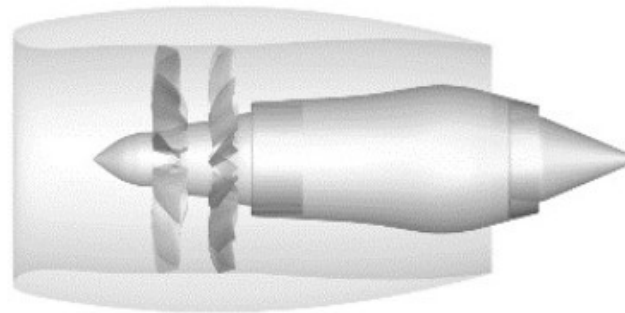


CFD airplane,
A320 type



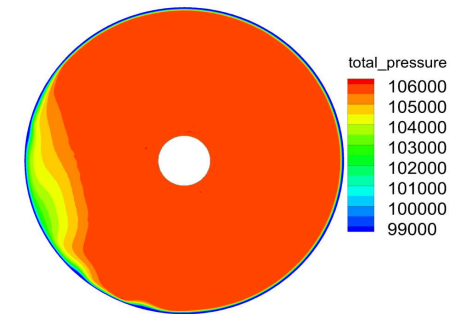
length 37.57 m
 wing surface 122 m²
 span width 34 m

UHBR engine,
CR turbo-fan

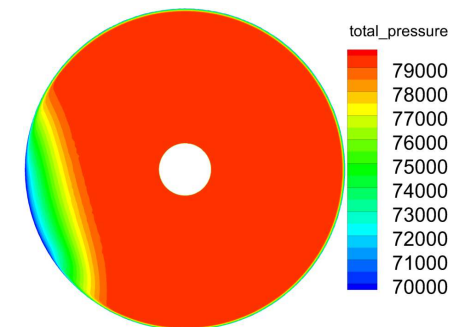


fan diameter 2.343 m
 blade numbers 10/12
 bypass ratio 17:1

embedding grade 30%, Take-Off



embedding grade 15%, Climb



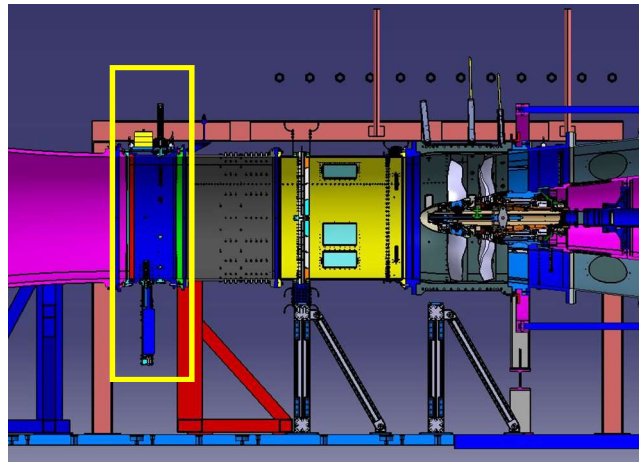
Test bench and Fan rig



settling chamber



fan inlet and outlet



CRISPmulti
(Counter Rotating Integrated
Shrouded Propfan)

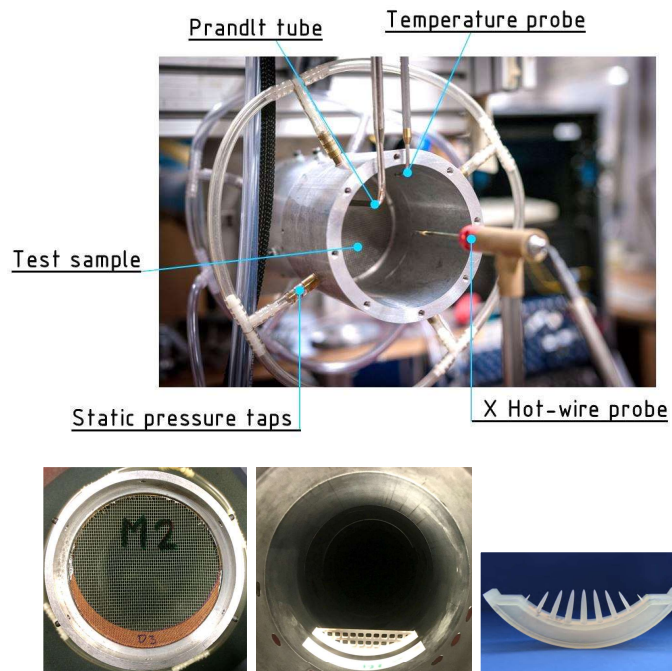


Multi-stage 2-shaft compressor test bench M2VP at DLR Cologne

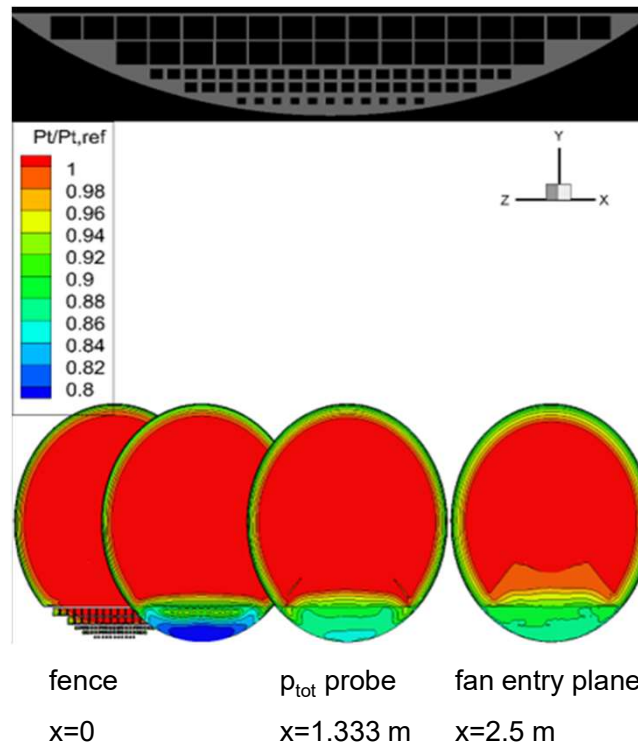
carbon composite blades
fan diameter 1 m
blade numbers 10/12
PR @ ADP 1.3
mass flow@ADP 159 kg/s

Development of inflow distortion device (IFD)

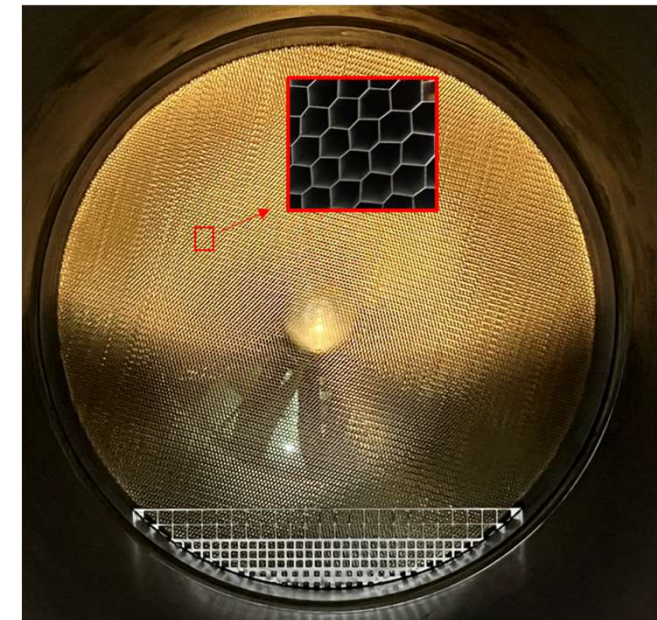
Testing of IFD effectiveness at high-speed windtunnel



CFD optimization of fence perforation



Traversable distortion fence used at M2VP combined with honey comb



TEST CAMPAIGN 2022

Multi-disciplinary test campaign May-June 2022



Aerodynamics

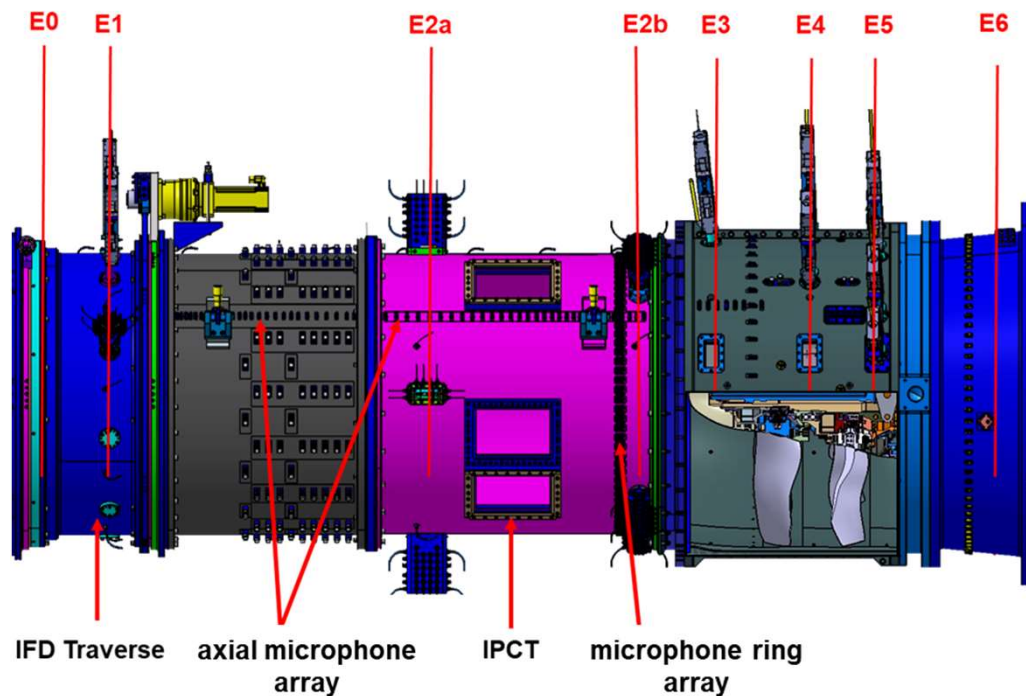
- total pressure rakes,
total temperature rakes,
boundary layer rakes
- 5-hole probes,
- instationary pressure sensors
- hotwire anemometry
- particle image velocimetry (PIV)

Aeroelastics, Structure

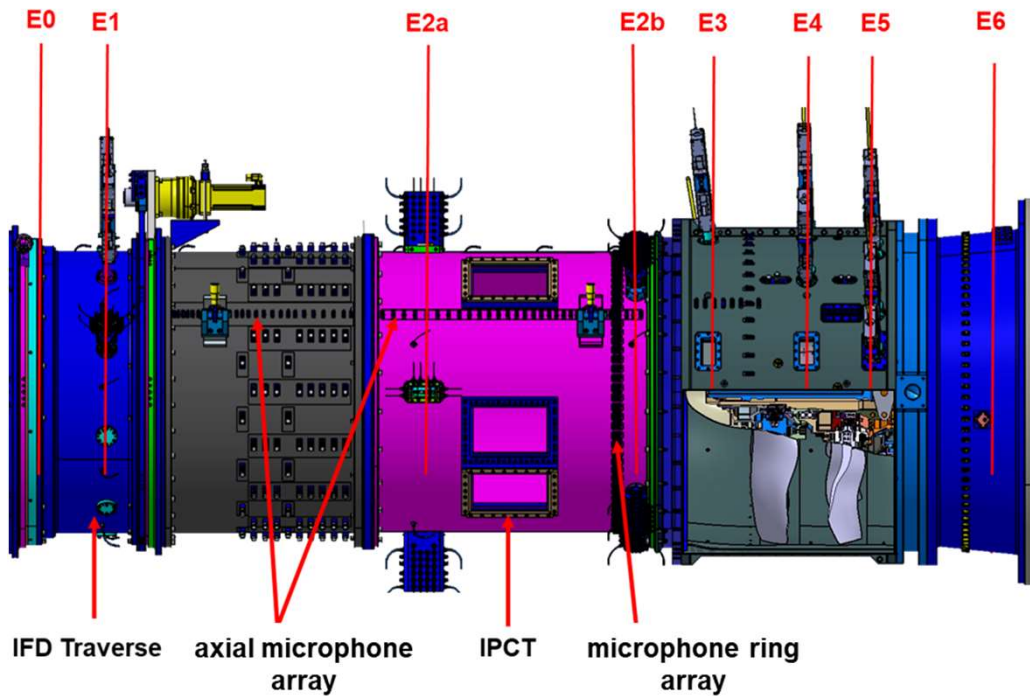
- Image Pattern Correlation
Technique
- DMS, BSSM

Acoustics

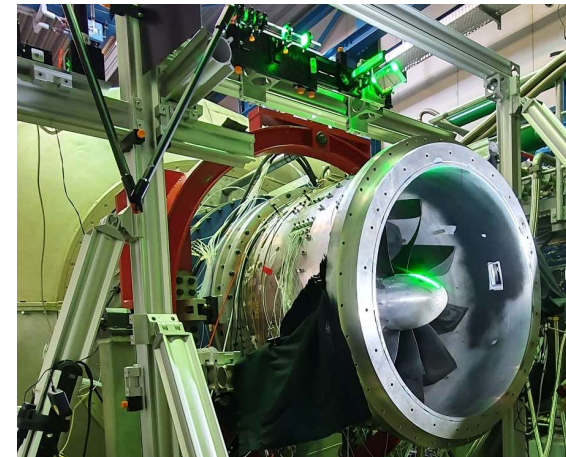
- microphone arrays



Multi-disciplinary test campaign May-June 2022



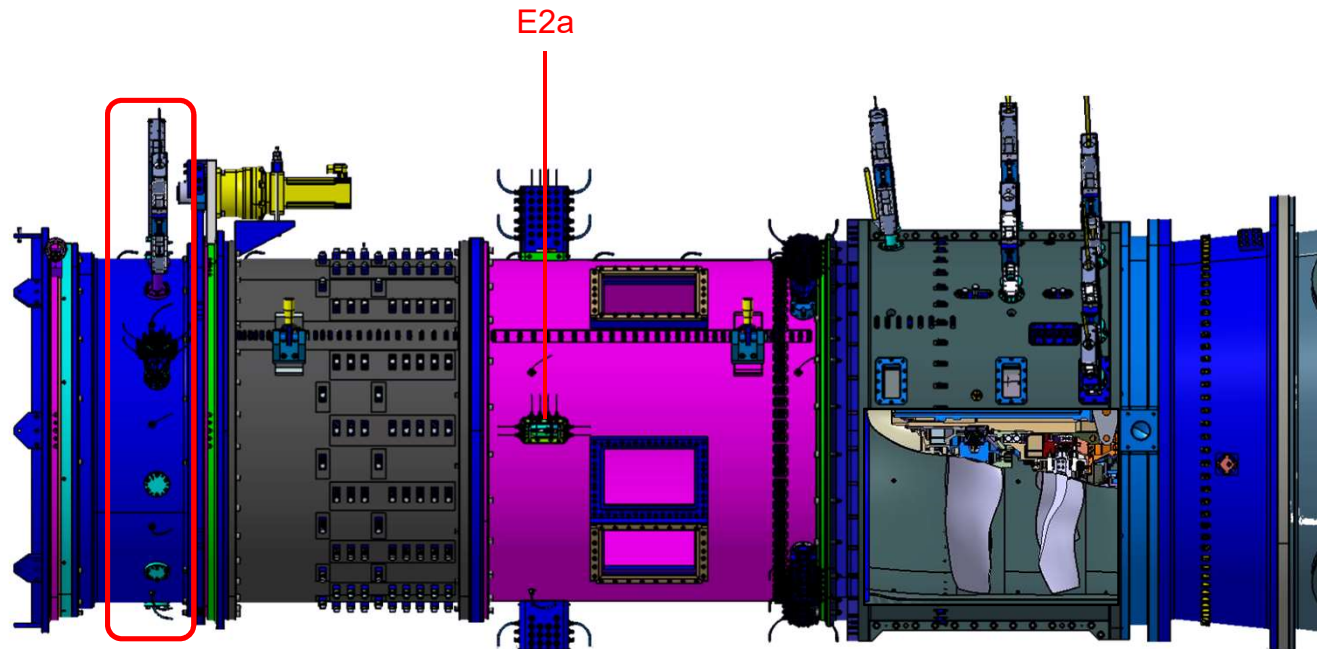
Stereo PIV of mean flow



Optical measurement of blade displacements and deformations

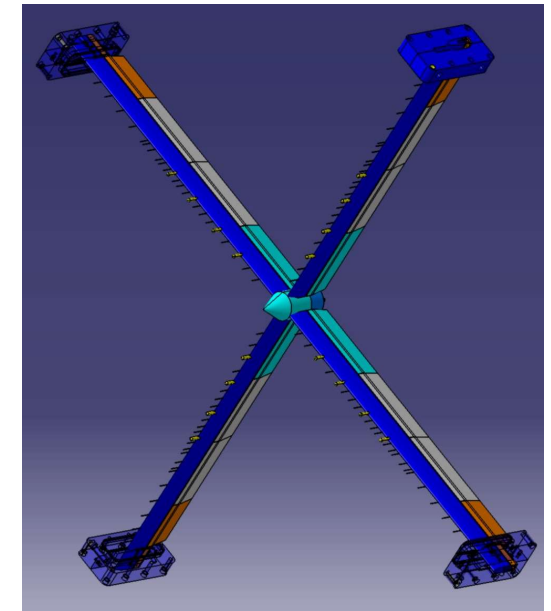


Measurement of total pressure distribution of fan inflow

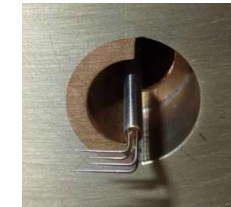
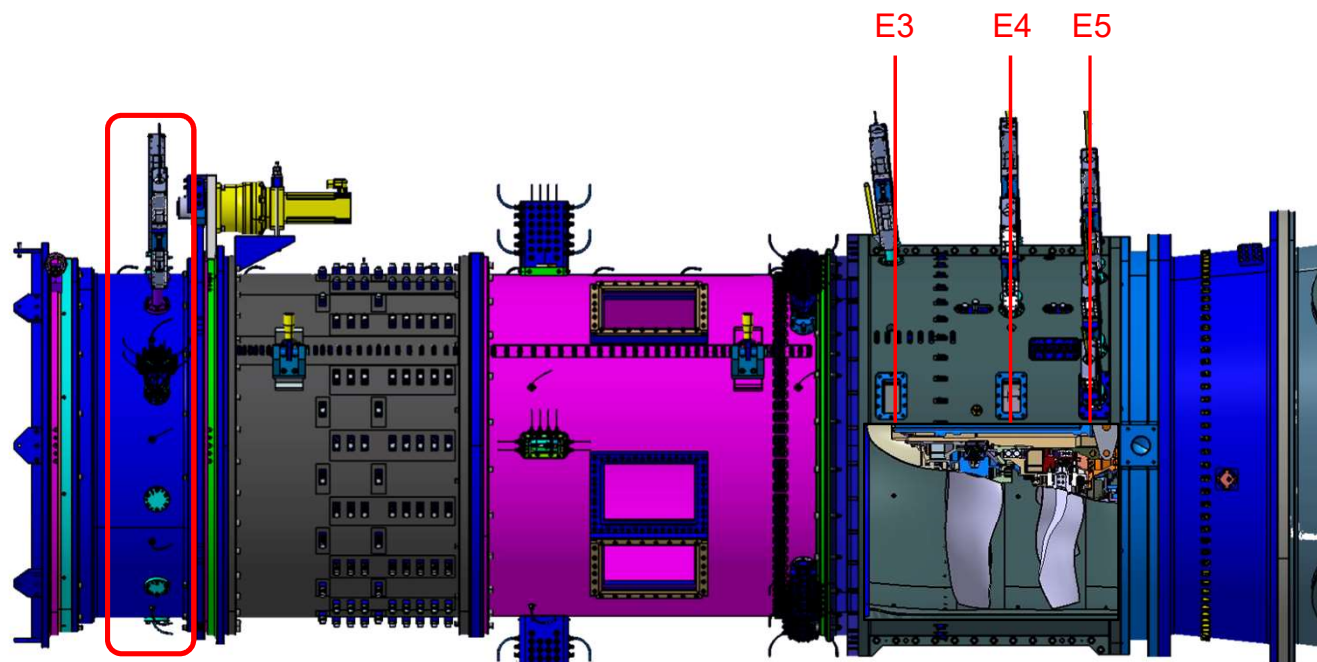


inflow distortion
device

fan



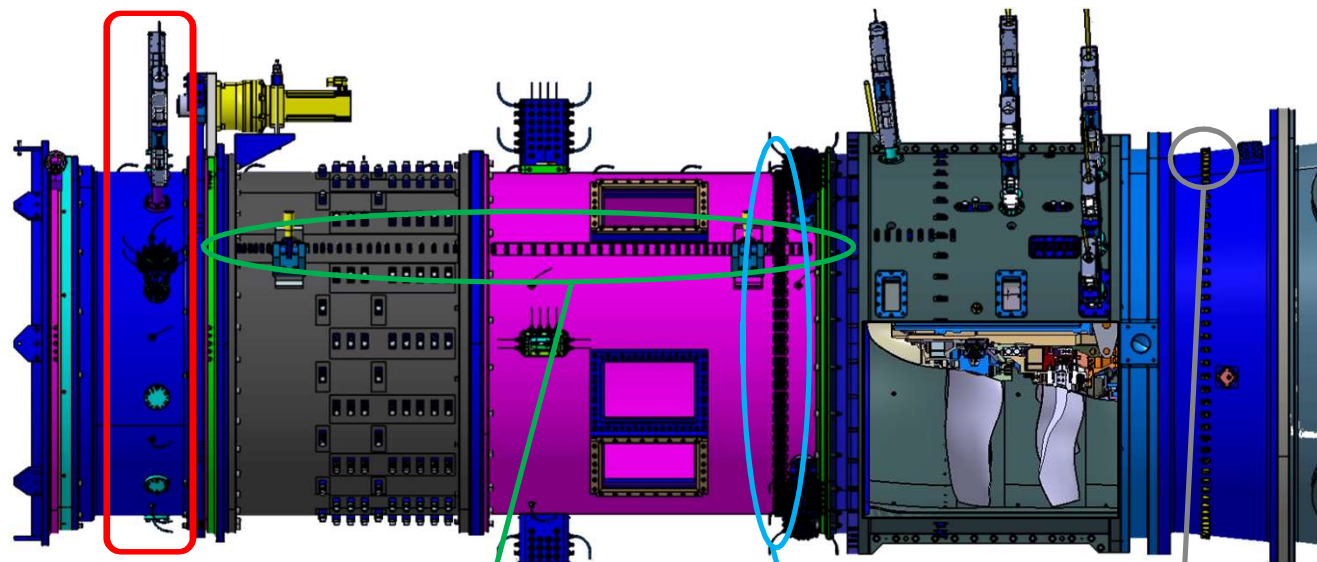
Hotwire measurements upstream / interstage / downstream of fan



inflow distortion
device

fan

Acoustic measurements upstream / downstream of fan



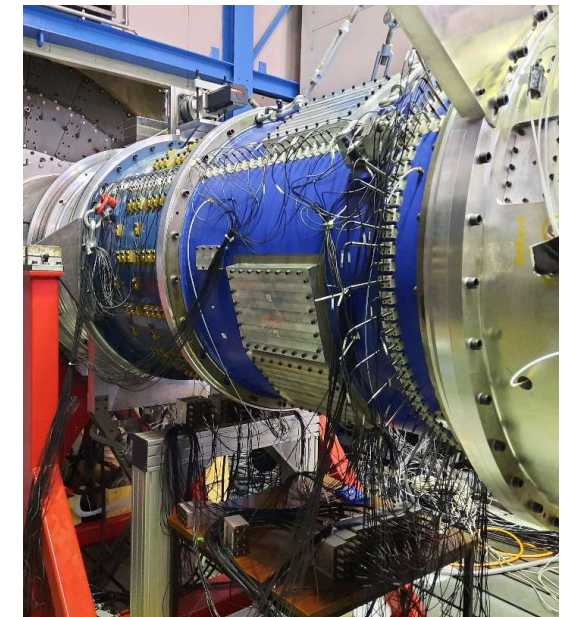
inflow distortion
device

mic line array

mic ring array

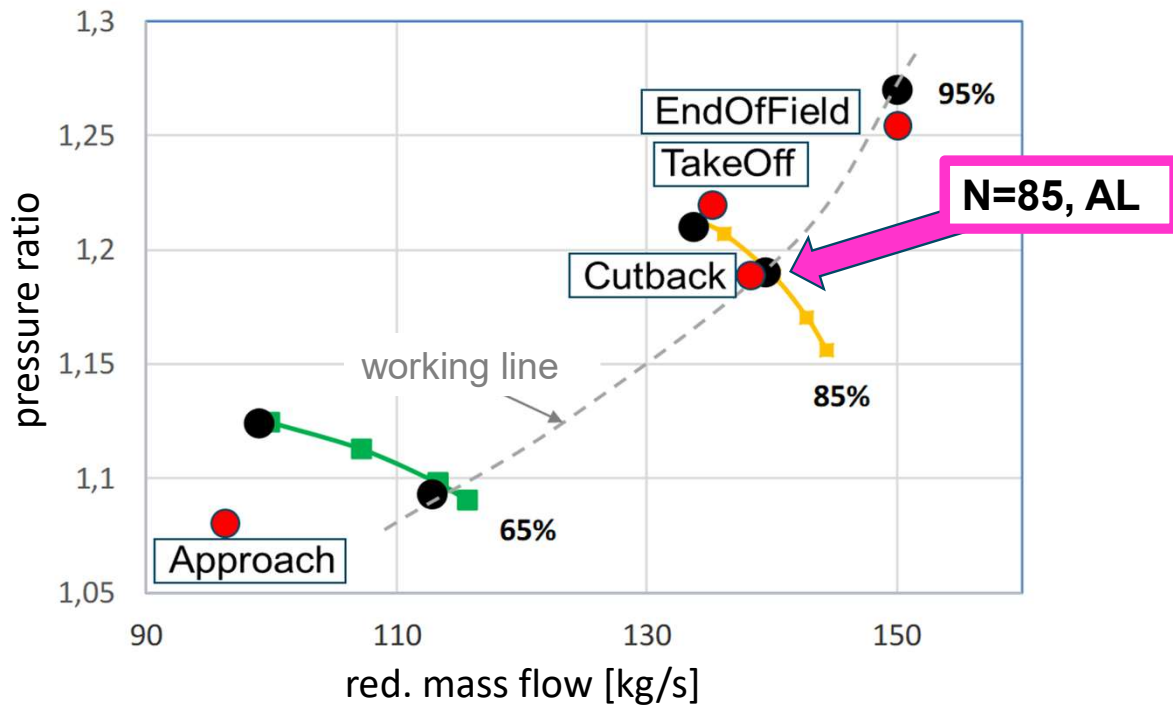
fan

3 mics



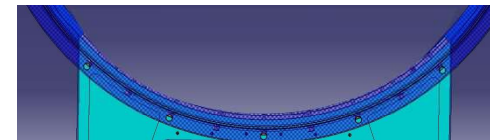
SOME RESULTS

Selected fan operating points with BLI

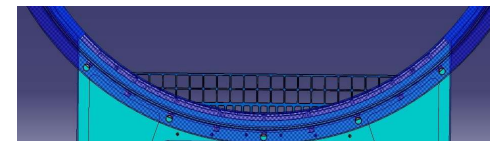


- measured OP
- acoustic relevant OP

distortion fence variation



ZH = 0 mm



ZH = 70 mm



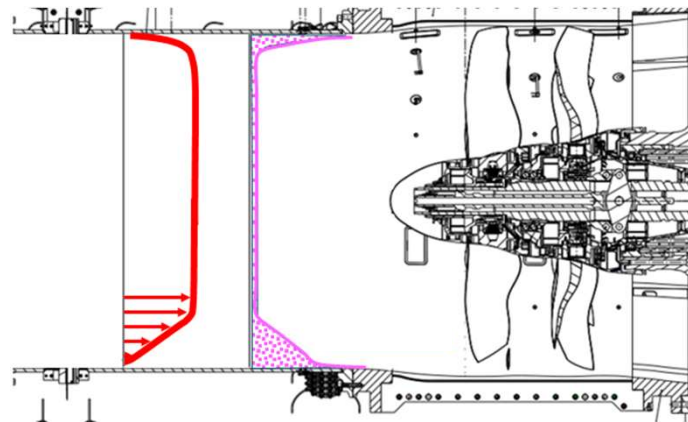
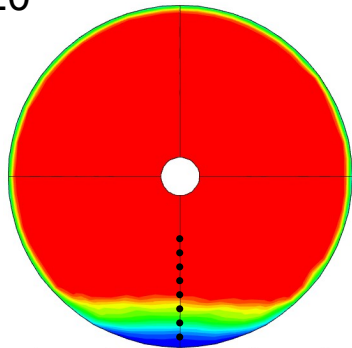
ZH = 120 mm

ZH = Zaun-Höhe = fence height

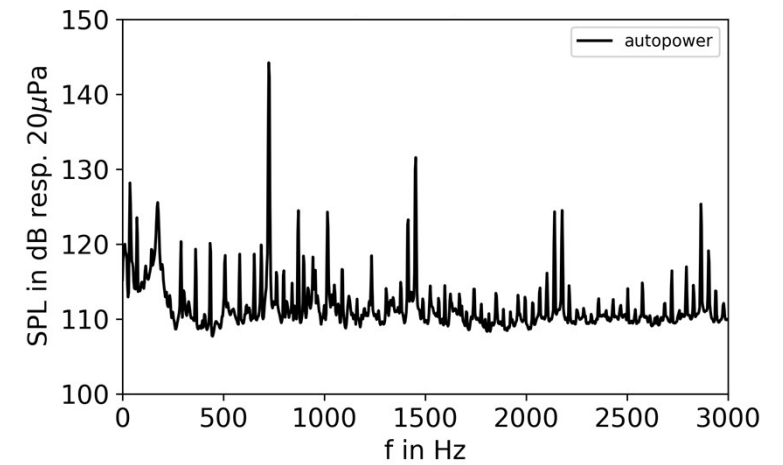
Goal: Assess BLI impact on four fan noise components



N=85,AL
ZH=120

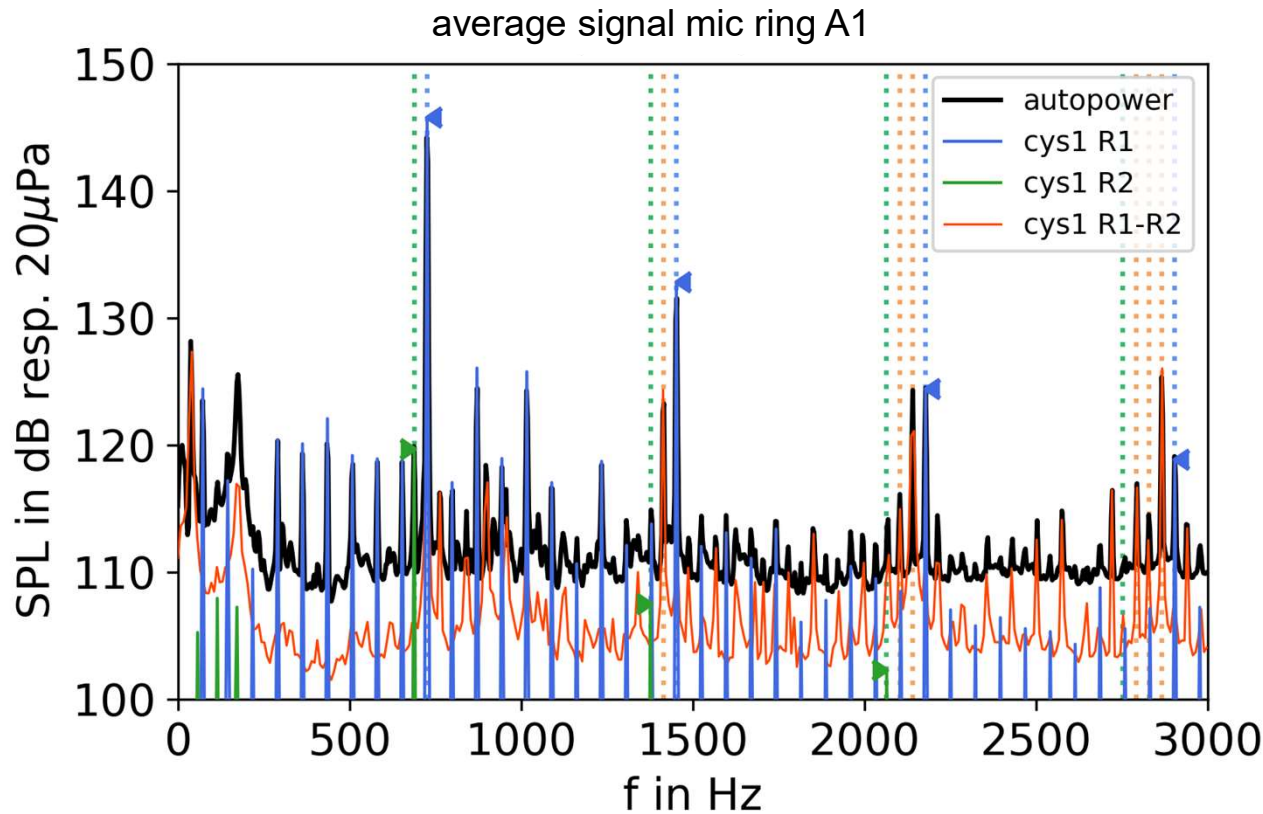


average signal mic ring A1



Noise components separated by cyclostationary analysis

N=85, AL, distortion fence 120 mm



rotor 1 blade tones @ $f = h_1 B_1 f_{rot1}$

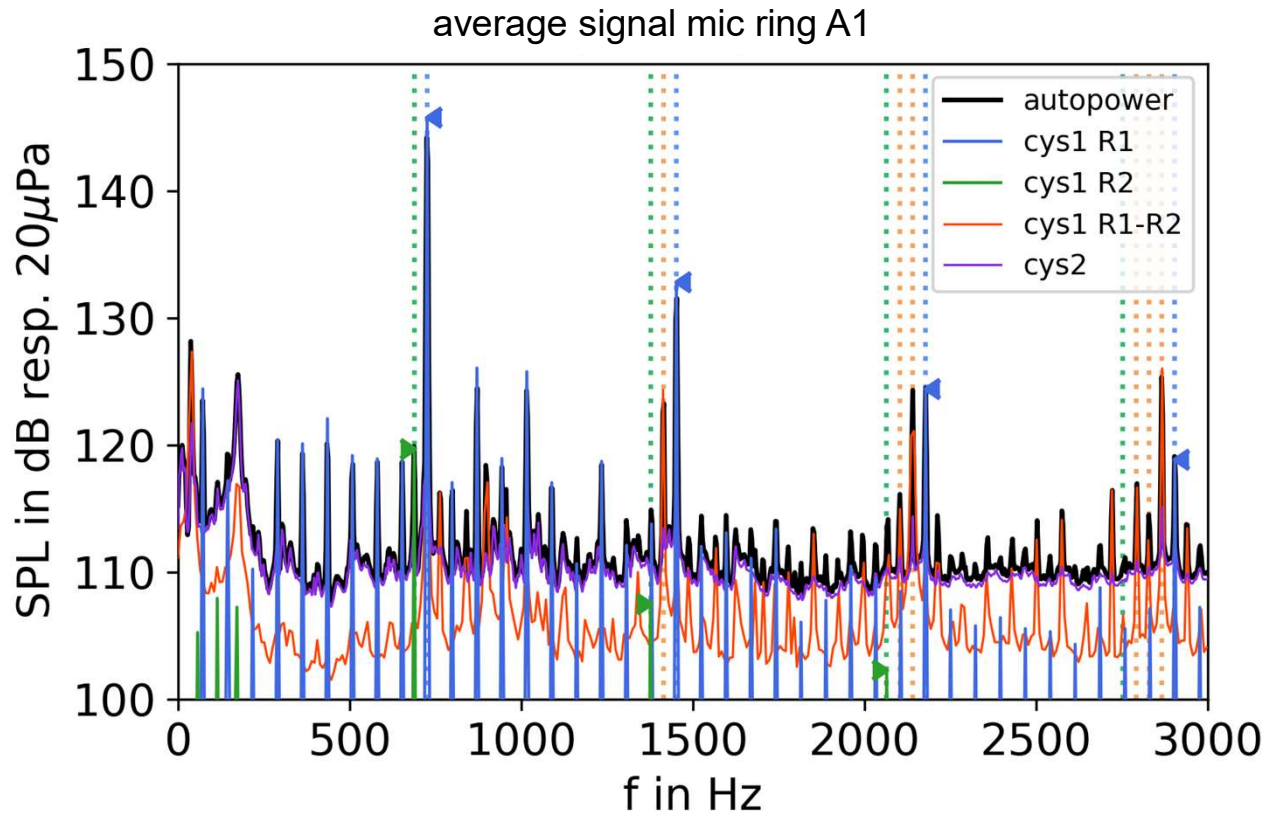
rotor 2 blade tones @ $f = h_2 B_2 f_{rot2}$

rotor 1 x rotor 2 interaction tones

@ $f = h_1 B_1 f_{rot1} + h_2 B_2 f_{rot2}$

Noise components separated by cyclostationary analysis

N=85, AL, distortion fence 120 mm



rotor 1 blade tones @ $f = h_1 B_1 f_{rot1}$

rotor 2 blade tones @ $f = h_2 B_2 f_{rot2}$

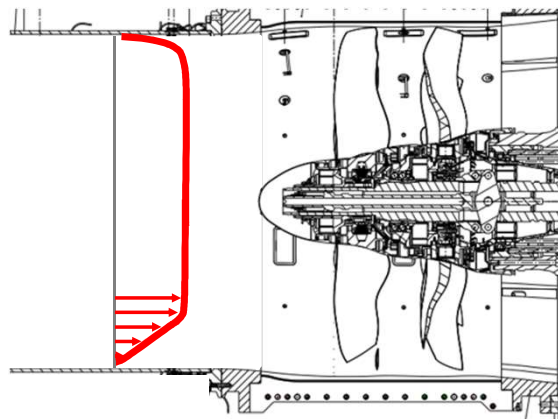
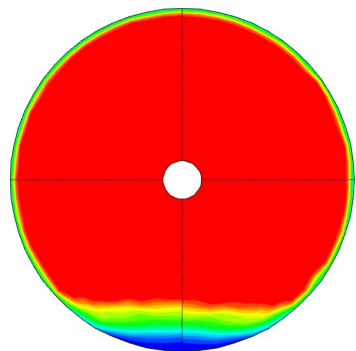
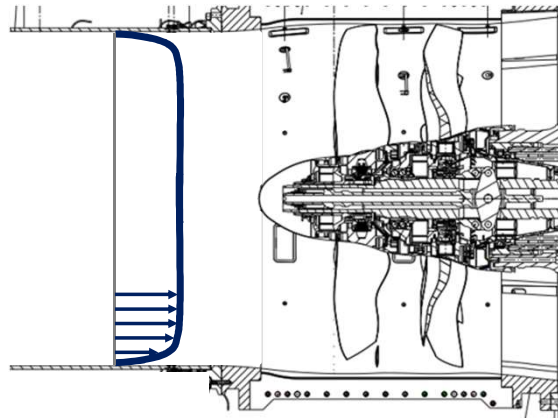
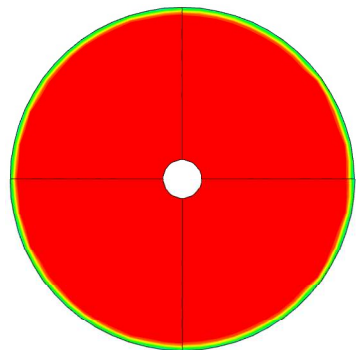
rotor 1 x rotor 2 interaction tones

$$@ f = h_1 B_1 f_{rot1} + h_2 B_2 f_{rot2}$$

rotor incoherent components

BLI impact on blade tones rotor 1 and rotor 2

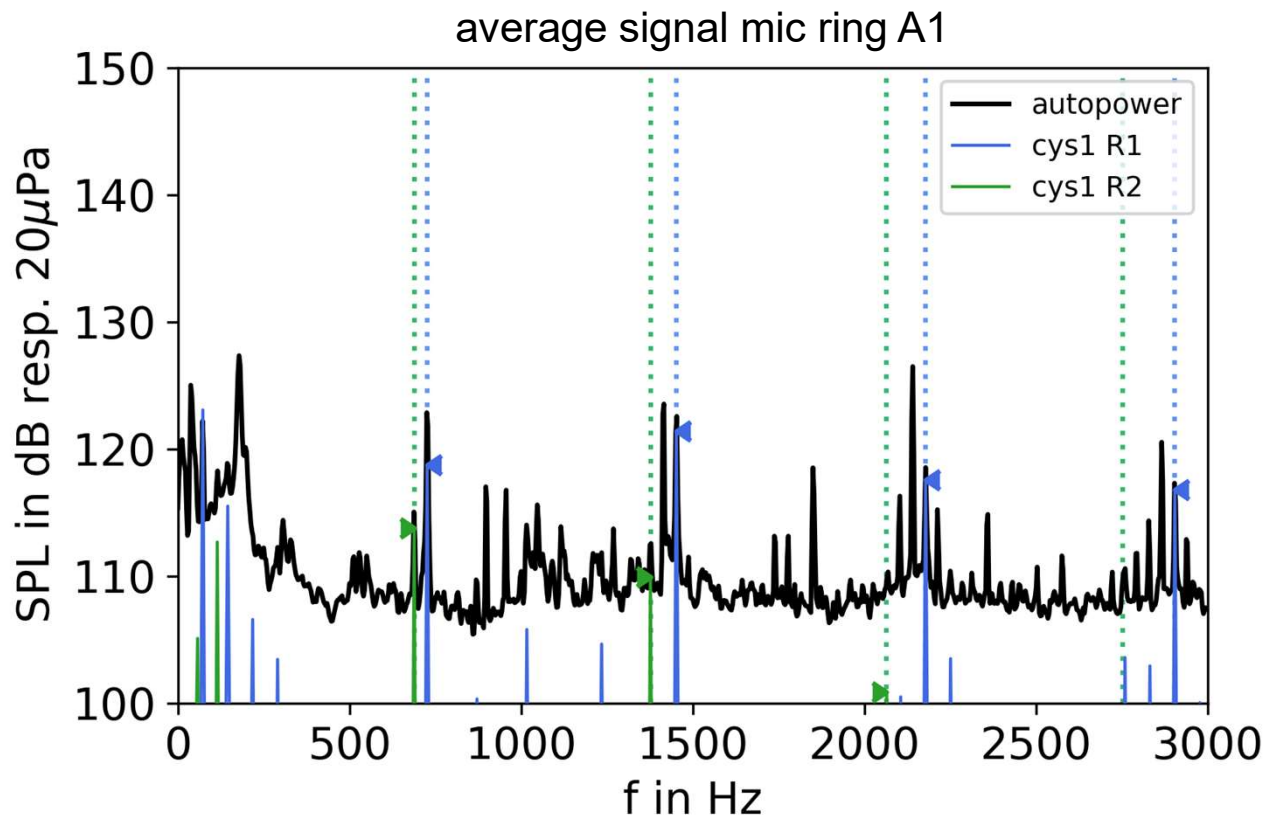
main noise generating mechanisms



- **Steady blade forces in uniform steady flow**
→ acoustically cut-off at subsonic operation
- (buzz saw tones at supersonic fan operation)

- **Unsteady blade forces due to interaction with non-uniform steady flow**
- (modification of buzz saw noise sources at super sonic fan operation)

Blade tones of rotor 1 and rotor 2 N=85, AL, without distortion fence

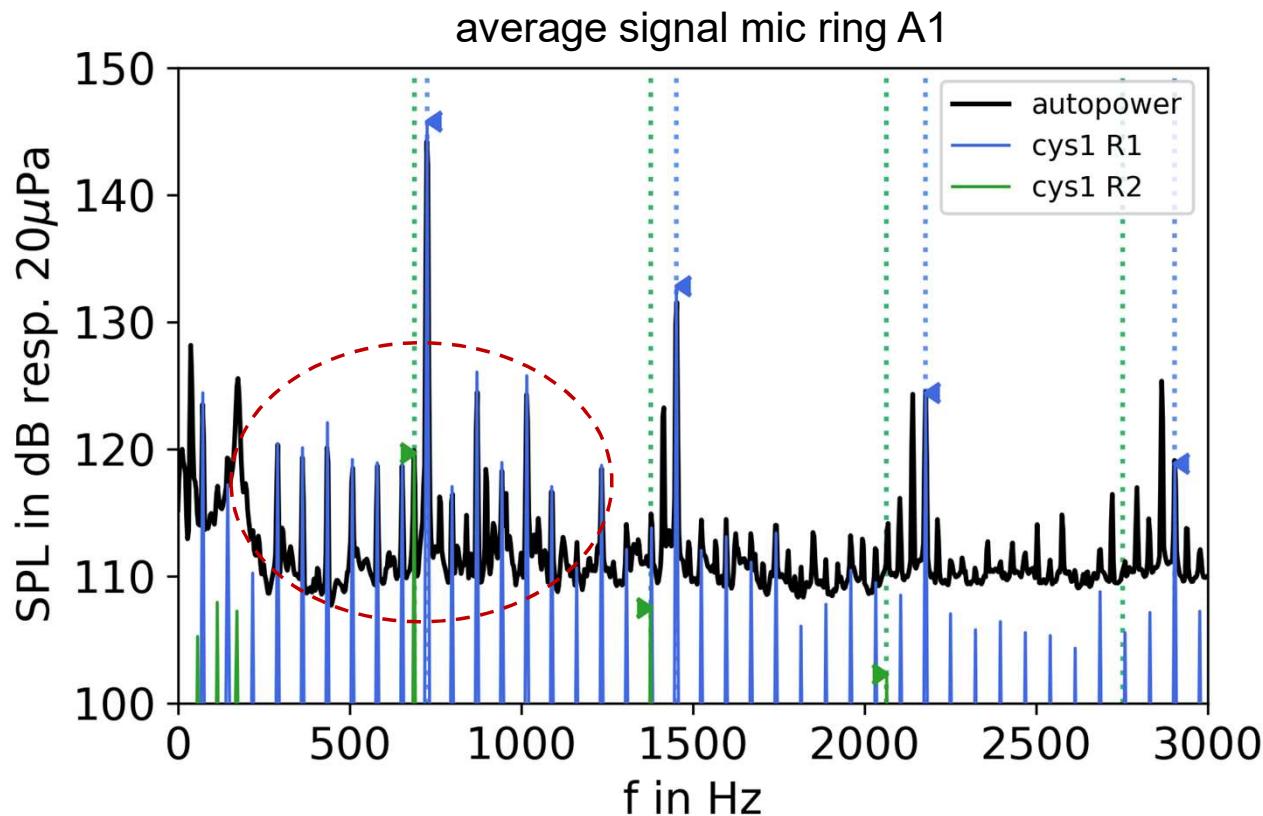


rotor 1 blade tones @ $f = h_1 B_1 f_{rot1}$

rotor 2 blade tones @ $f = h_2 B_2 f_{rot2}$

Blade tones of rotor 1 and rotor 2

N=85, AL, with distortion fence 120 mm

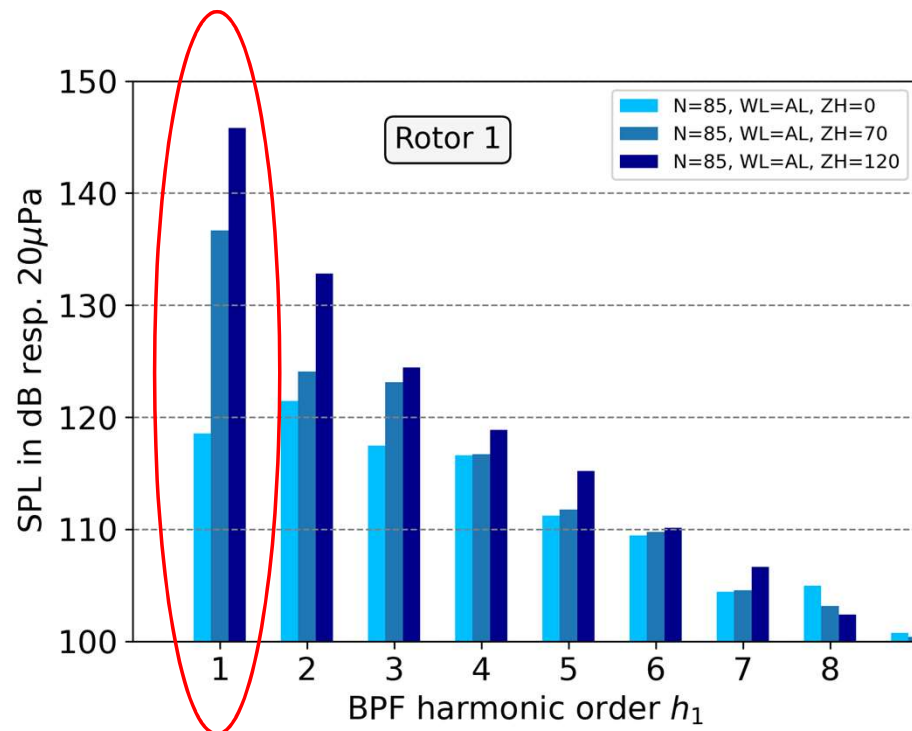


rotor 1 blade tones @ $f = h_1 B_1 f_{rot1}$

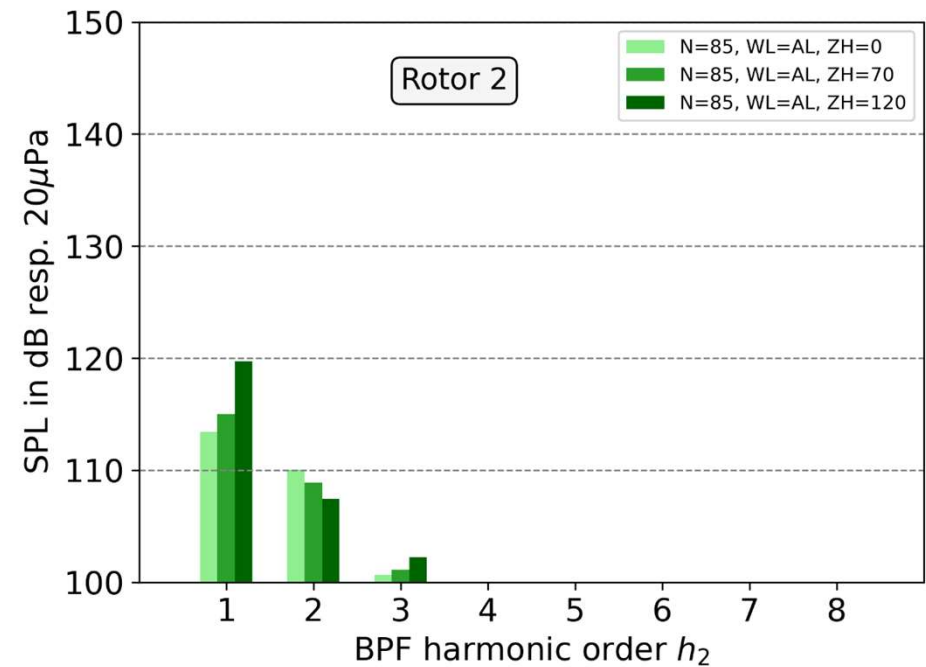
rotor 2 blade tones @ $f = h_2 B_2 f_{rot2}$

engine order harmonics due to blade deformations caused by BLI?

BLI impact on blade tones rotor 1 and rotor 2 N=85, AL

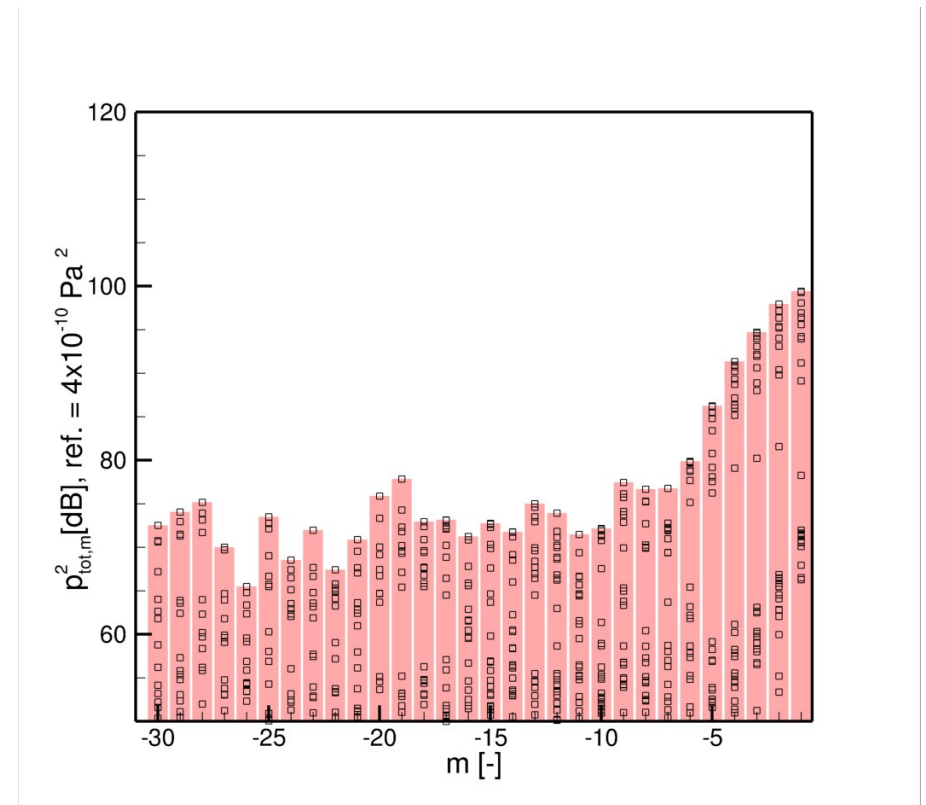
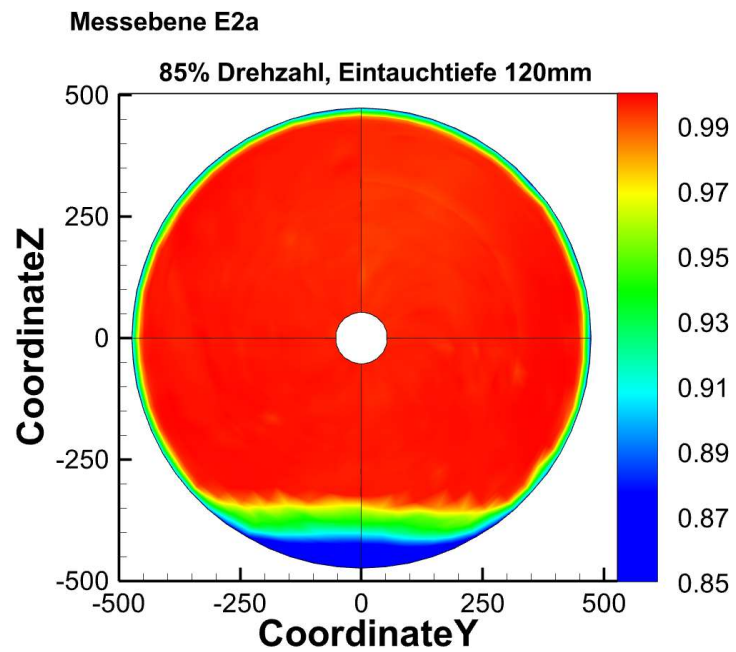


strong aerodynamic excitation at low orders



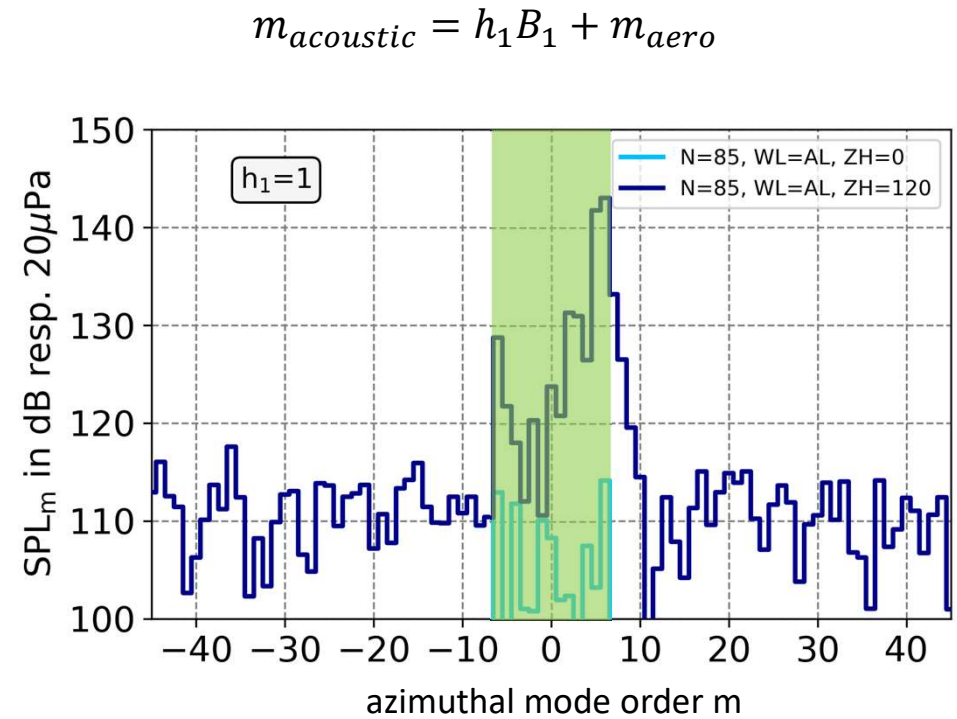
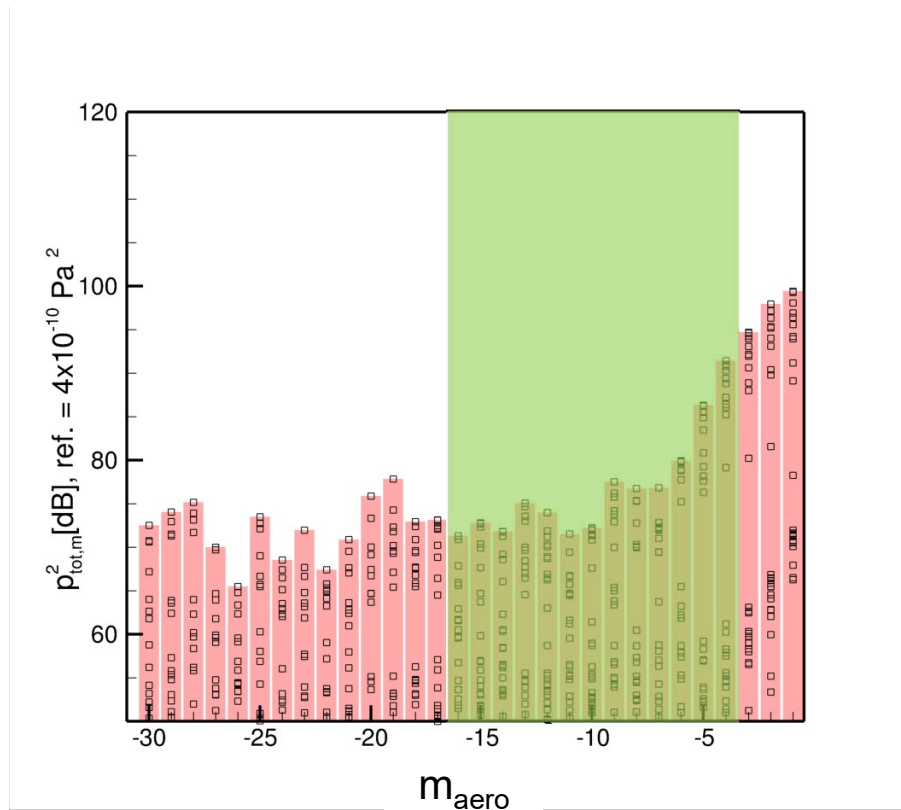
interaction BLI / rotor 2 is subordinate

Inflow distortion decomposed into circumferential modes



Relation of aerodynamic and acoustic modes

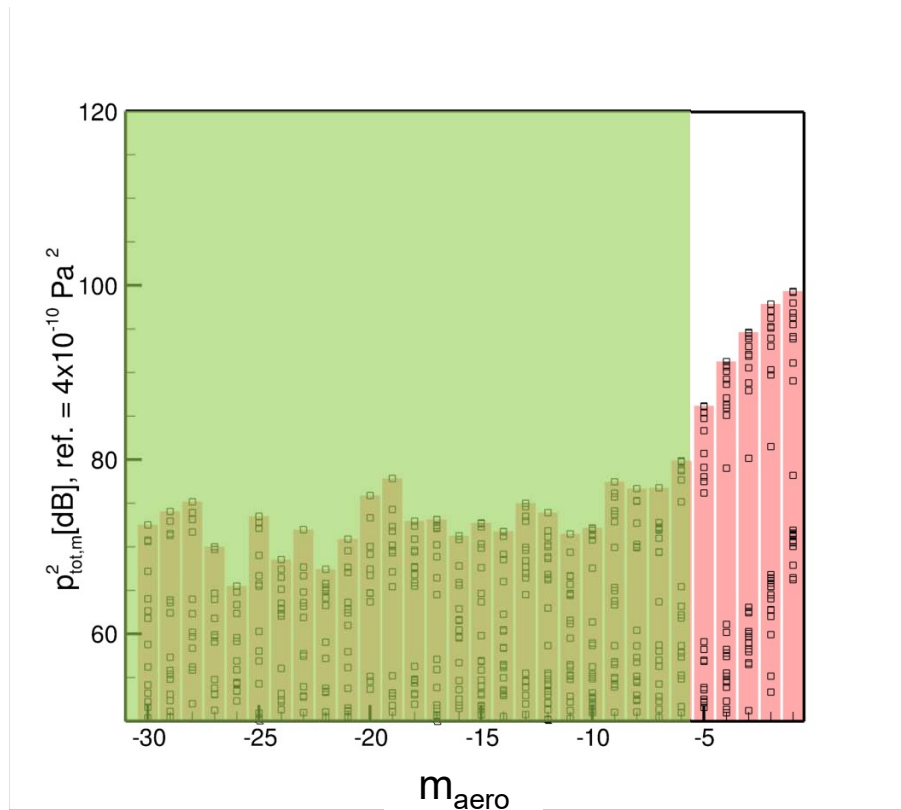
N=85, AL, 1BPF1



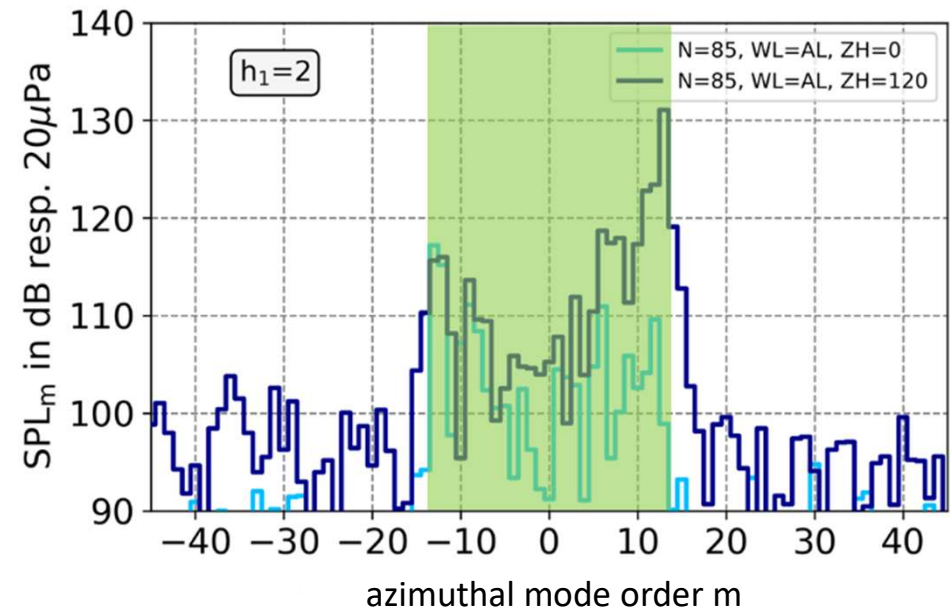
- level increases of aerodynamic and acoustic modes correlate
- asymmetrical mode excitation due to alignment of the dipole sources
- resonance and propagation effects to be considered

Relation of aerodynamic and acoustic modes

N=85, AL, 2BPF1

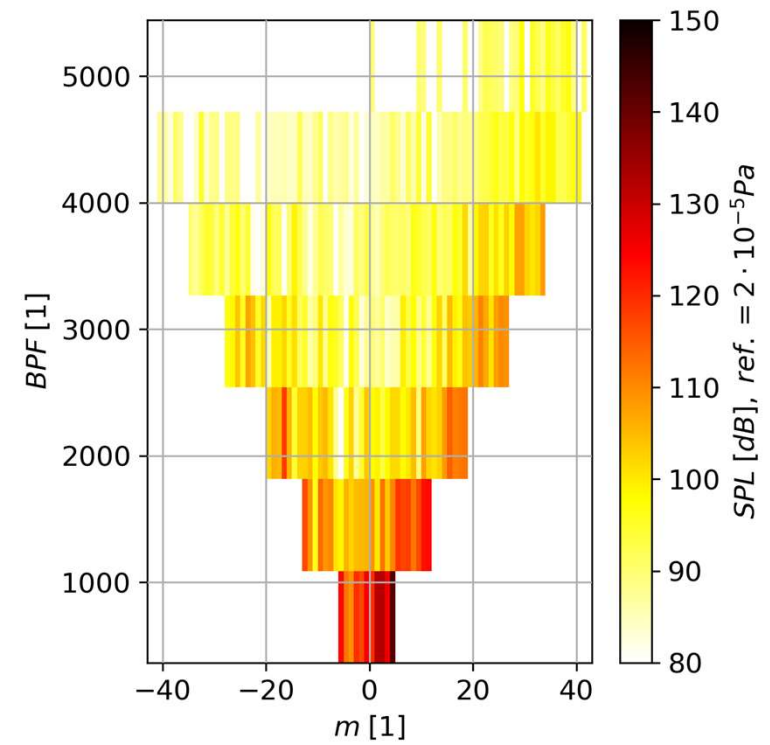
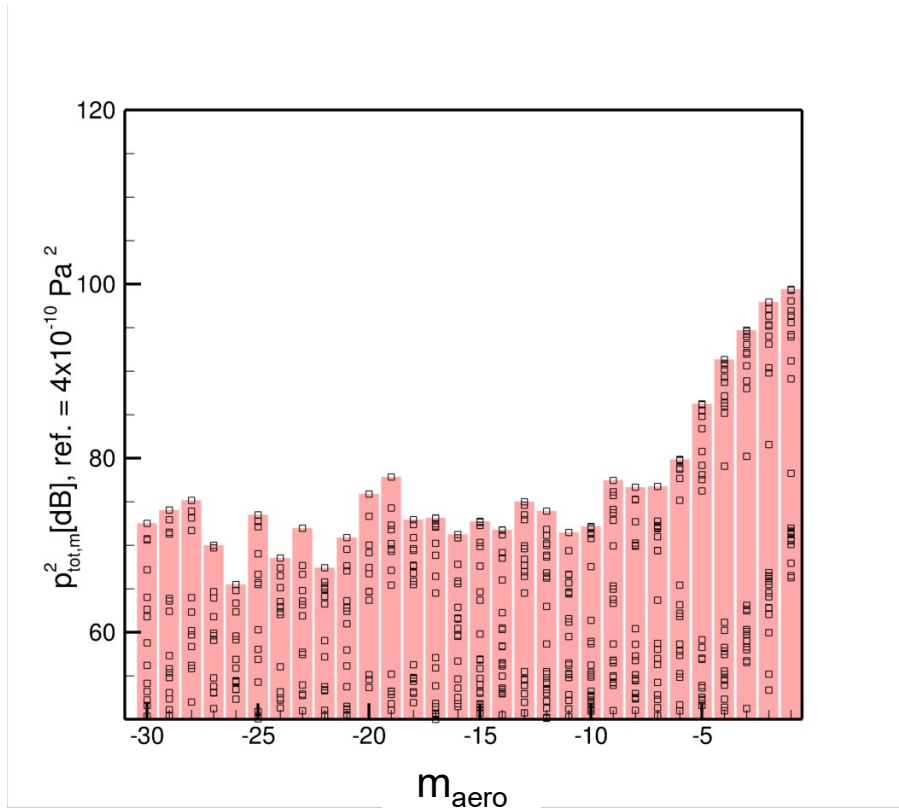


$$m_{acoustic} = h_1 B_1 + m_{aero}$$



Relation of aerodynamic and acoustic modes

N=85, AL, hBPF1



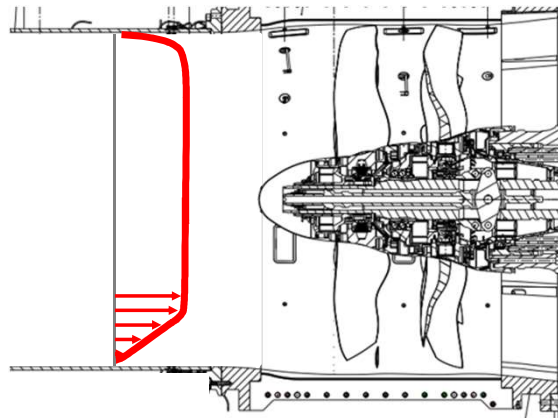
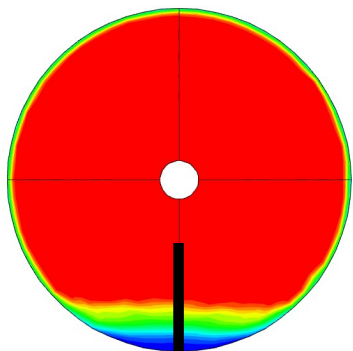
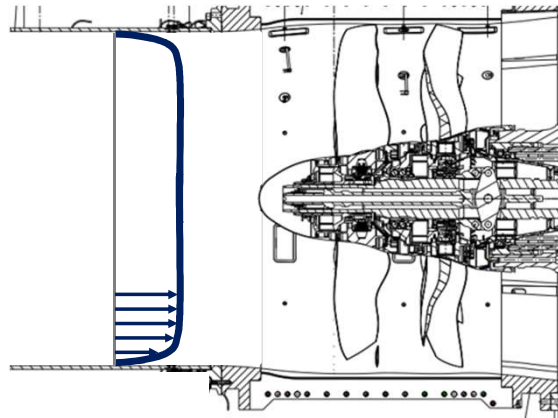
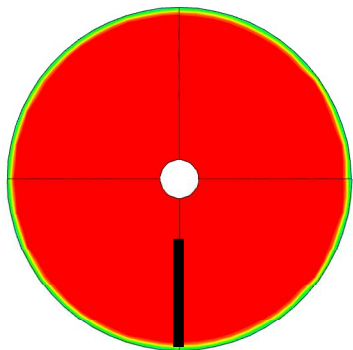
BLI impact on rotor 1/rotor 2 interaction tones

main noise generating mechanisms

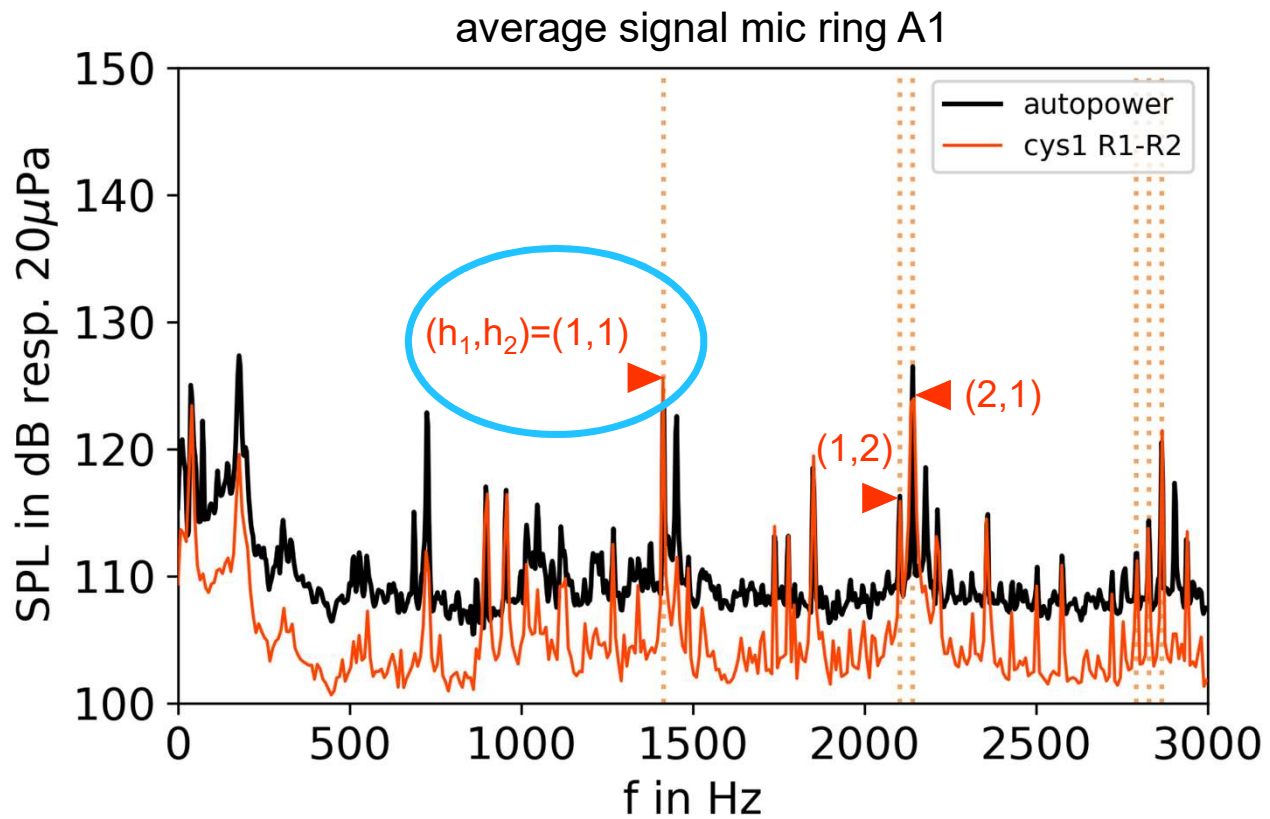
- interaction rotor 1 wakes / rotor 2
 - interaction potential fields rotor 1 / rotor 2
- interaction modes according to Tyler&Sofrin

$$m = h_1 B_1 - h_2 B_2$$

- rotor 1 wakes vary during rotation
 - potential fields of rotor blades vary during rotation
- generation of modes adjacent to Tyler&Sofrin modes



Separation of rotor 1/rotor 2 interaction tones N=85, AL, no distortion fence



tones rotor 1 x rotor 2

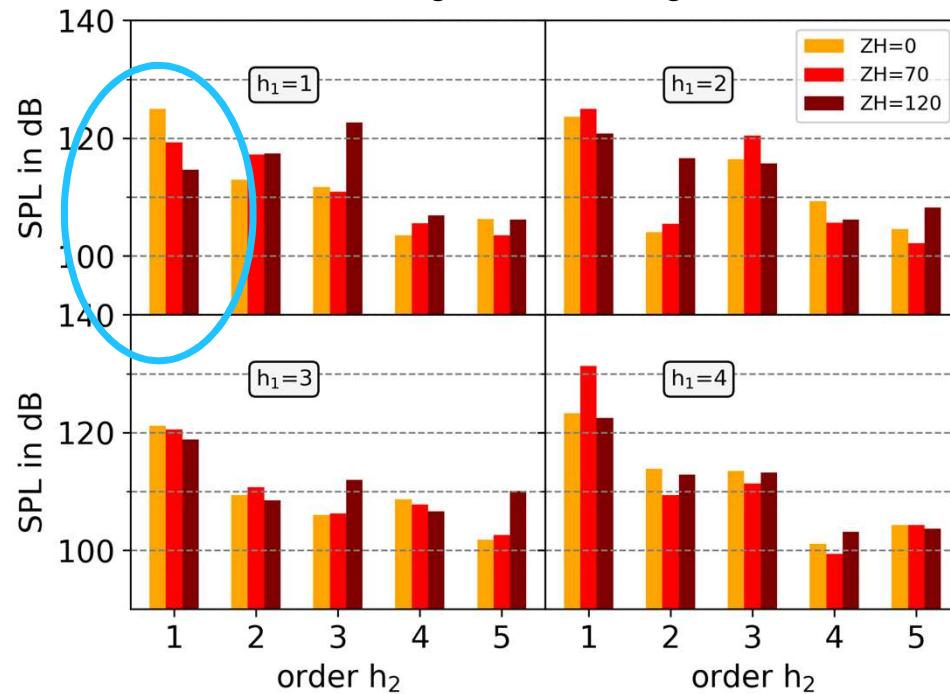
$$@ f = h_1 B_1 f_{rot1} + h_2 B_2 f_{rot2}$$

BLI impact on rotor 1/rotor 2 interaction tones

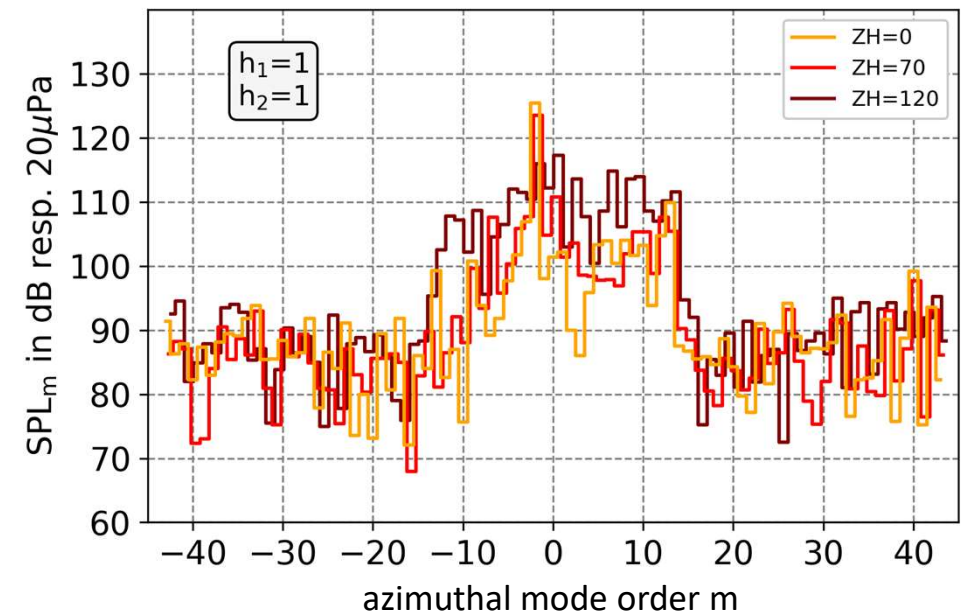
N=85, AL



average tones in ring A1



azimuthal modes in ring A1



- BLI modifies blade wake and potential field
- blade deformations may have an impact
- propagation effects to be considered

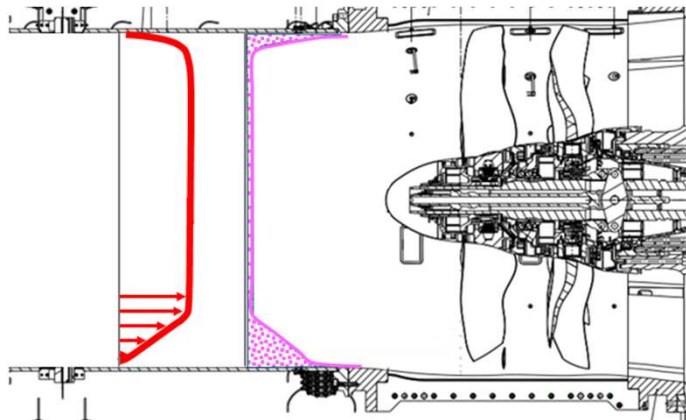
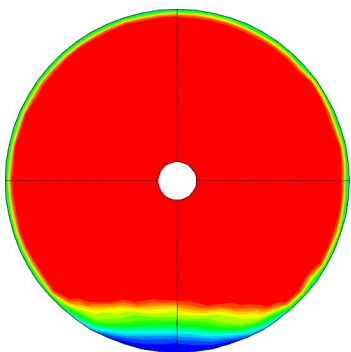
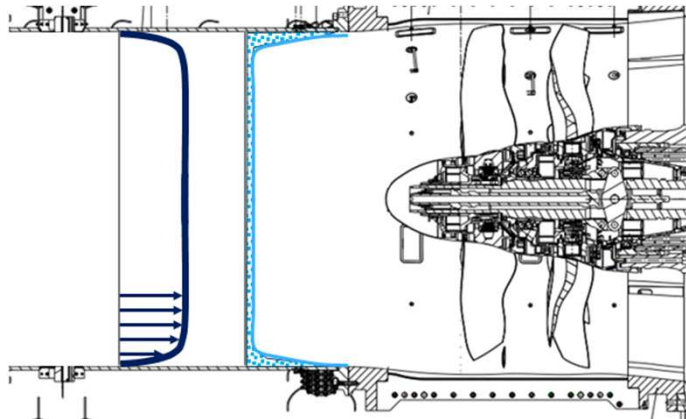
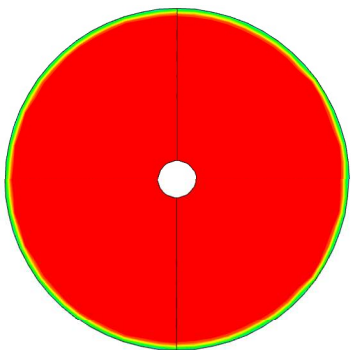
BLI impact on rotor-incoherent noise sources

main noise generating mechanisms

turbulence interaction

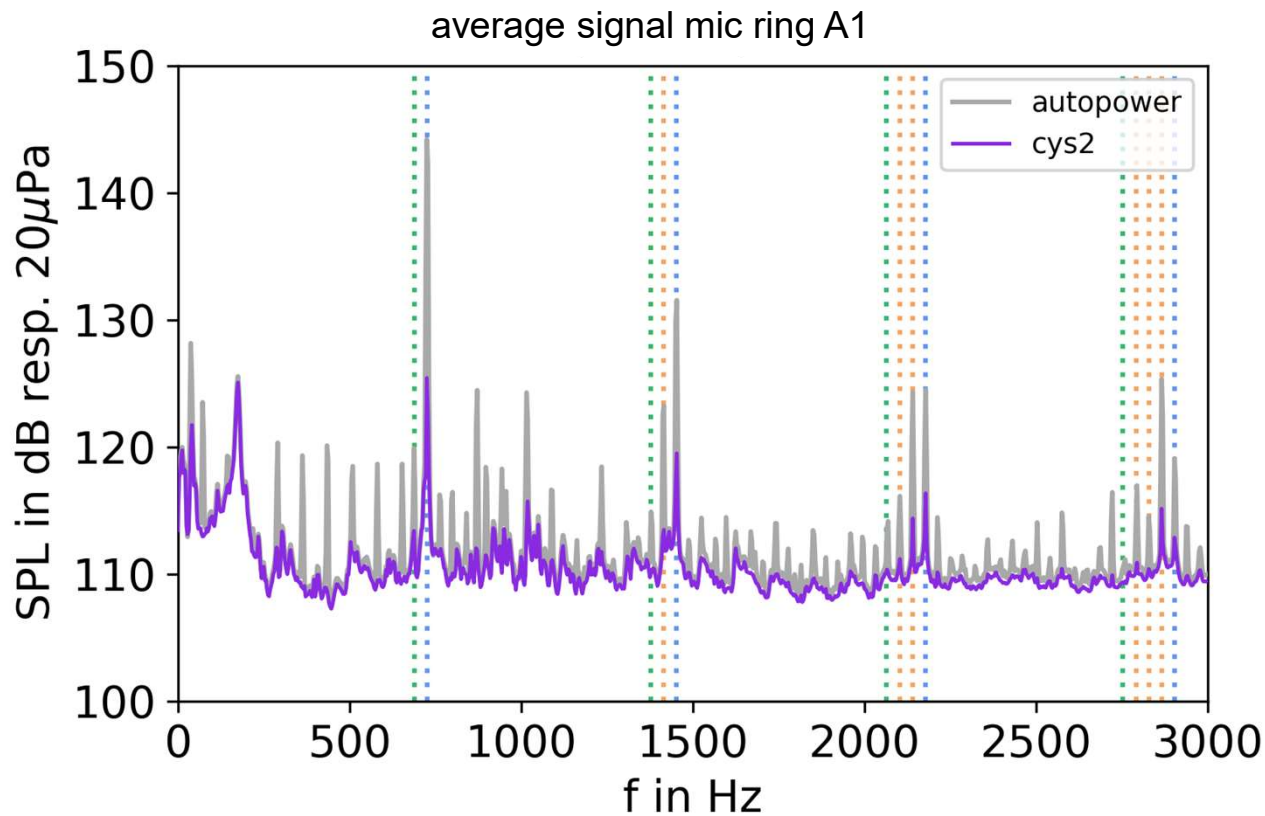
- inflow → rotors
- rotor 1 wakes → rotor 2
- rotor blade tip vortices → rotor 2

- modification of aforementioned mechanisms
- BLI → rotor 1 and rotor 2



Separation of rotor incoherent signal components

N=85, AL, distortion fence 120 mm



tones rotor 1 @ $f = h_1 B_1 f_{rot1}$

tones rotor 2 @ $f = h_2 B_2 f_{rot2}$

tones rotor 1 x rotor 2

@ $f = h_1 B_1 f_{rot1} + h_2 B_2 f_{rot2}$

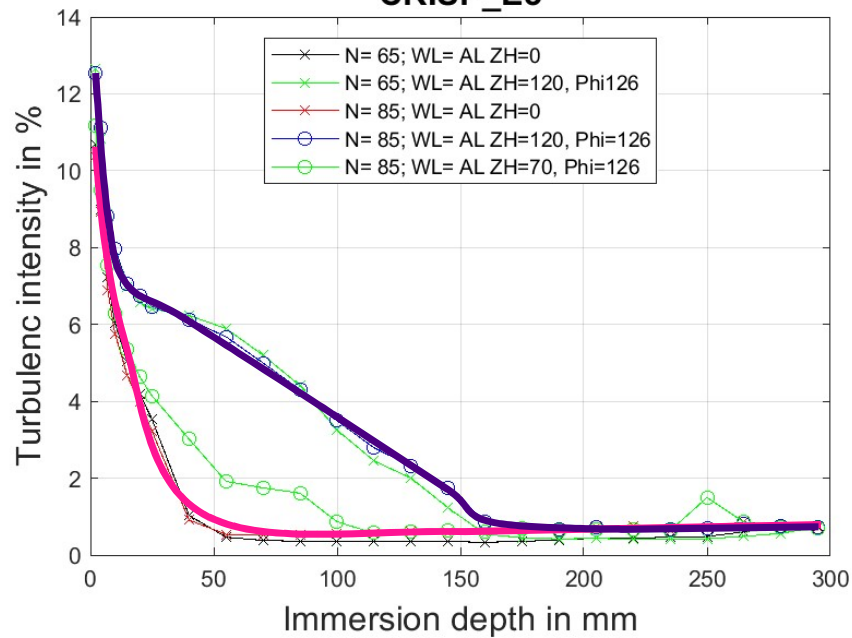
rotor incoherent signal

BLI impact on rotor-incoherent noise sources

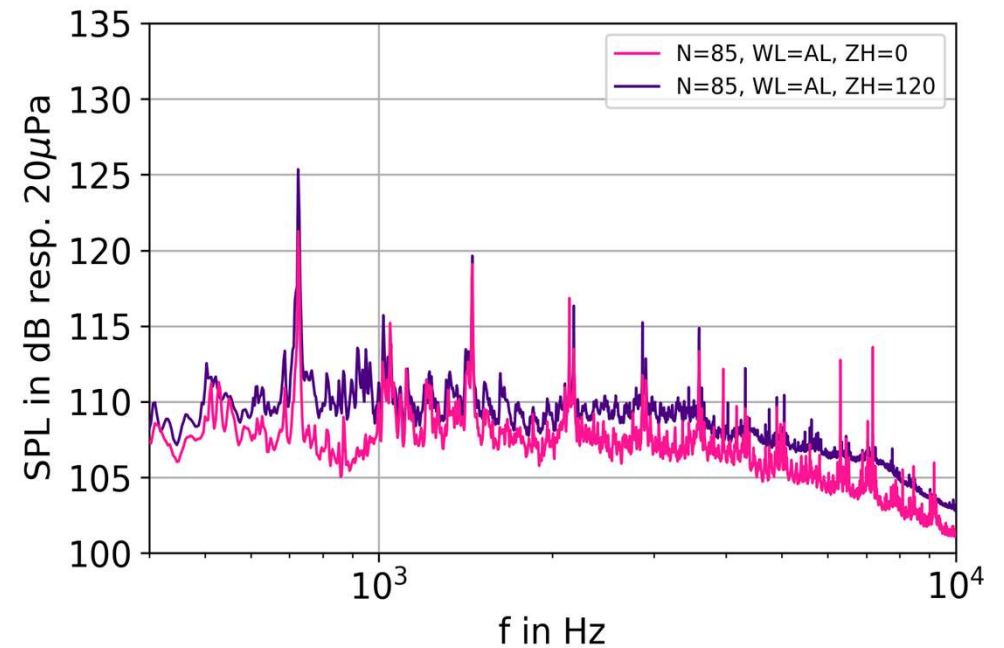
N=85, AL



HW1 Turbulence intensity, filtered in axial direction
CRISP_E3

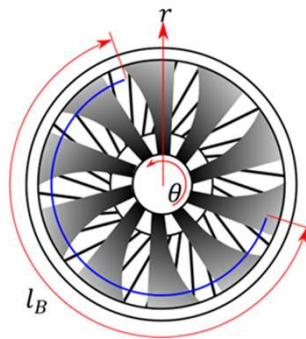
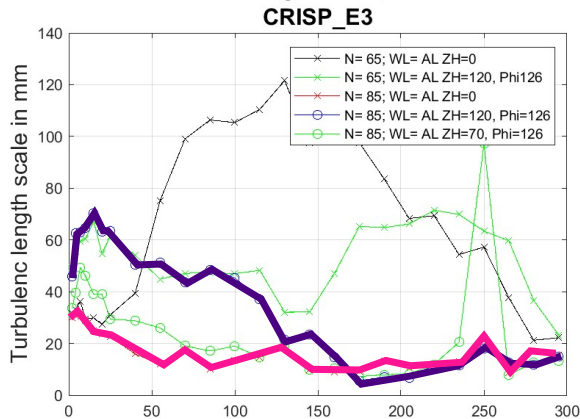


average signal mic ring A1

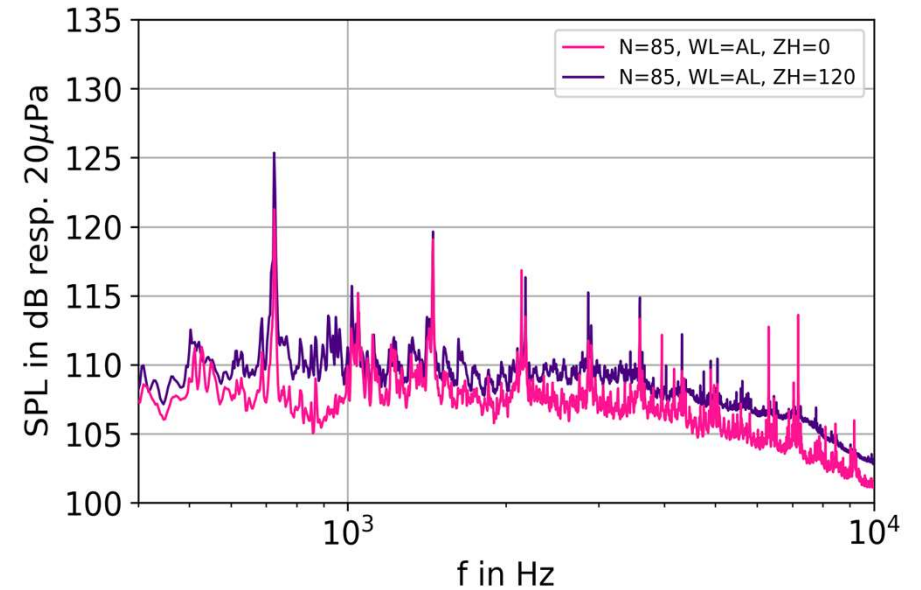


Relation to turbulence length scales N=85, AL

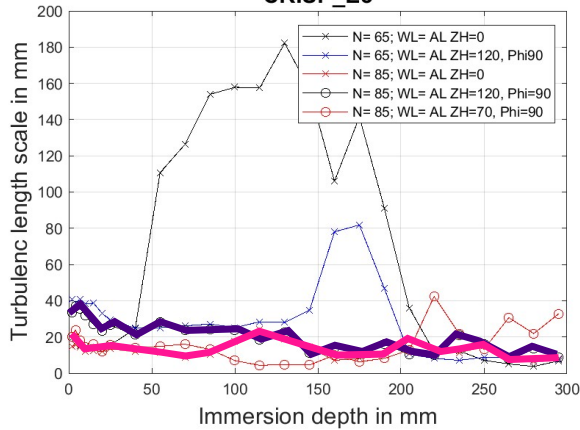
HW1 Turbulence length scale, in axial direction



average signal mic ring A1



HW2 Turbulence length scale, in tangential direction
CRISP_E3



$$l_b = \sqrt{l_t^2 + \left(2\pi \frac{f_{rot} r}{U(r)} l_l\right)^2}$$

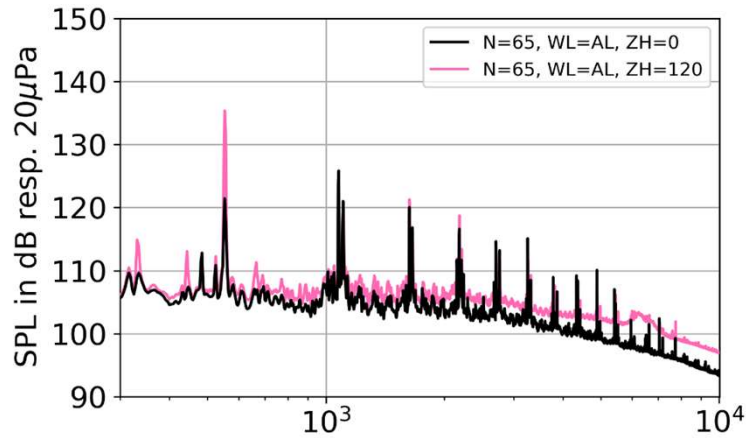
$$\frac{\text{coherence length } l_b}{\text{blade spacing } s} = 0.3$$

- sources of successive blades are not correlated
- no 'haystacking' around BPF harmonics
- how representative are length scales?

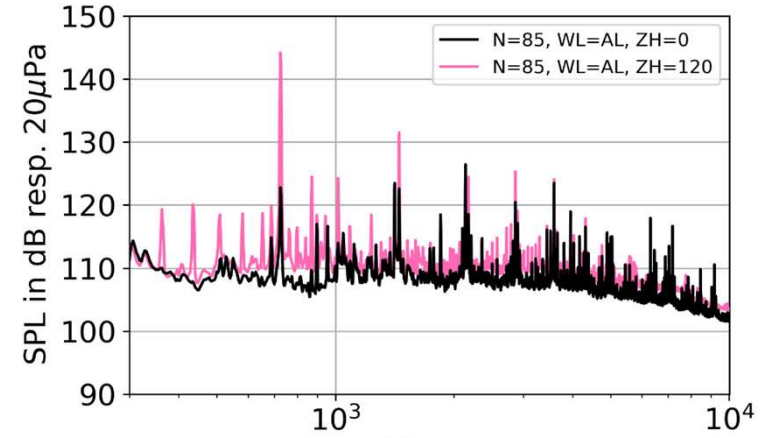
Overview of main measured test points average autopower spectra



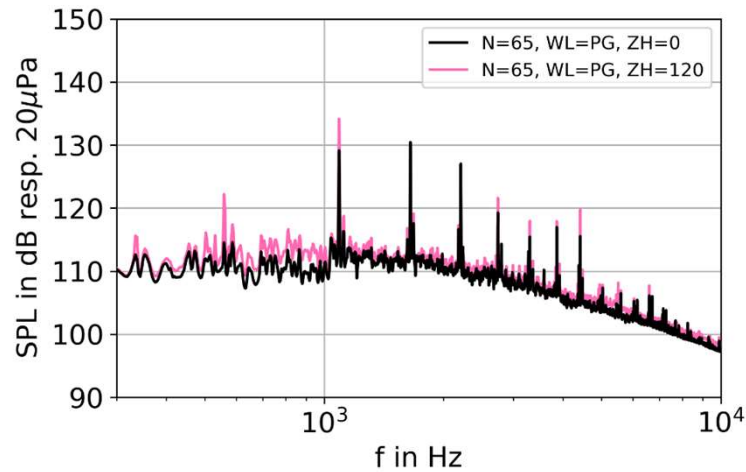
**N=65
AL**



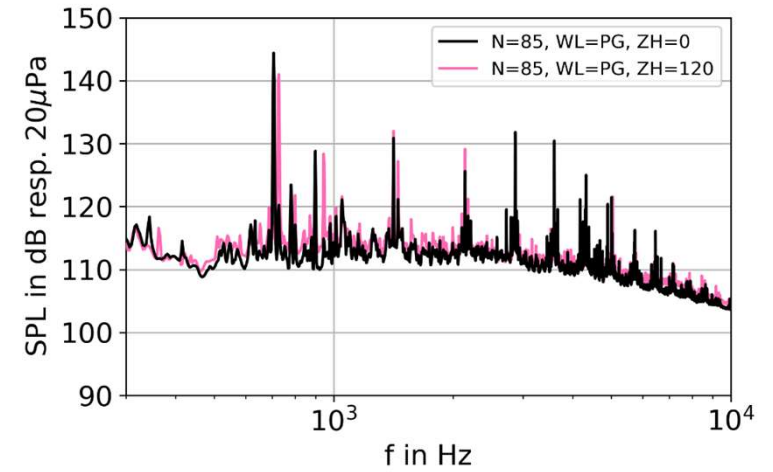
**N=85
AL**



**N=65
throttled**



**N=85
throttled**



Conclusion



- Comprehensive data base of tests under realistic engine conditions available
 - Aerodynamics, acoustics, blade deformations & vibrations
- Significant BLI effects on fan aeroacoustics measured
 - strong excitation of rotor 1 tones (isolated from other stage interactions)
 - modification of blade wake and potential field interaction of rotor 1 and rotor 2
 - rotor-incoherent excitation correlates well with turbulence intensity and length scales

Outlook / Ideas for further studies

- Paper at the AIAA/CEAS Aeroacoustics Conference 2024 in Rome
- Radial mode analysis under consideration of boundary layer profile
- Validation of fan noise prediction methods

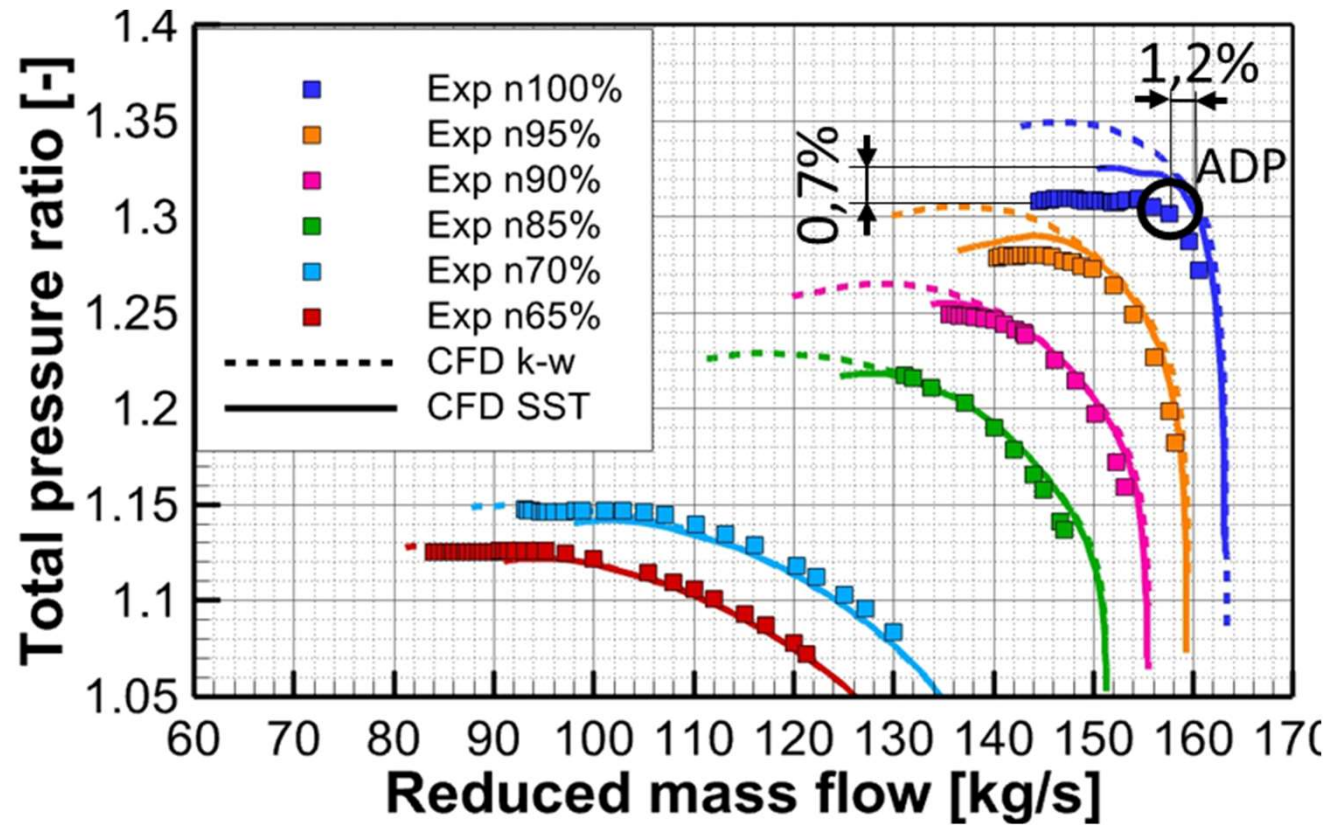
THANK YOU FOR YOUR ATTENTION

References



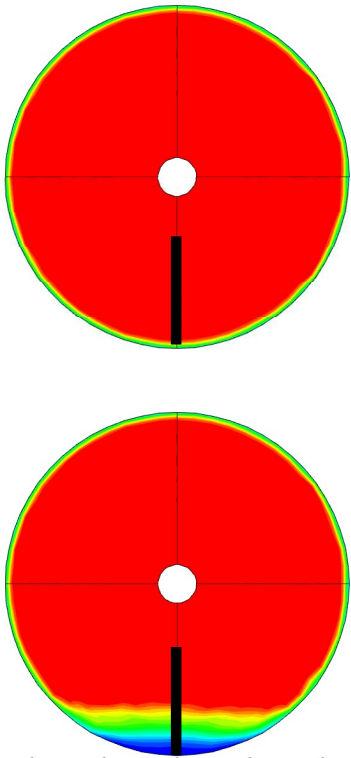
- Eichner, F., Belz, J., Winkelmann, P., Schnell, R., & Lengyel-Kampmann, T. (2019). Prediction of aerodynamically induced Fan Blade Vibration due to Boundary Layer Ingestion. *13th European Conference on Turbomachinery and Fluid Dynamics, ETC2019-370*
- Forsthofer, N., & Reiber, C. (2016). Structural Mechanic and Aeroelastic Approach for Design and Simulation of CFRP Fan Blades. *Deutscher Luft- und Raumfahrtkongress 2016, DLRK*. Braunschweig.
- Kajasa, B., Lengyel-Kampmann, T., & Meyer, R. (2022). Numerical and Experimental Design of a radial displaceable Inlet Distortion Device. *ISABE-2022-228*. Ottawa: ISABE.
- Klinner, J., Schroll, M., Lengyel-Kampmann, T., Belz, J., Eichner, F., Winkelmann, P., & C. Willert, C. (2022). Measurement of Aerodynamically Induced Blade Distortion on a Shrouded Counter-Rotating Prop-Fan. *20th International Symposium on Applications of Laser and Imaging Techniques to Fluid Mechanics*. Lisbon, Portugal.
- Lengyel-Kampmann, T., Karboujian, J., Charroin, G., & Winkelmann, P. (2023). Experimental Investigation Of An Efficient And Lightweight Designed Counter-Rotating Shrouded Fan Stage. *15th European Turbomachinery Conference on Turbomachinery Fluid Dynamics and Thermodynamics*. Budapest.
- Meyer, R., Tapken, U., Klähn, L., Behn, M., T. Lengyel-Kampmann (2024): Unsteady flow, turbulence and acoustic measurements on the counter-rotating DLR turbo fan stage CRISPMulti, with and without inlet distortions, ASME 2024 Turbomachinery Technical Conference & Exposition, London, UK, GT2024-124839, to be published
- Proskurov, S., Mößner, M., Ewert, R., & Lummer, M. D.-W. (2021). Fan noise shielding predictions with a coupled DG/FM-BEM method for installed aircraft engines. *AIAA Aviation Forum*. Virtual Event.
- Tapken, U., Lengyel-Kampmann, T., Belz, J., Stürmer, A., & Otten, T. (2022). Auswirkung von Grenzschichteinsaugung auf Akustik - Übersicht über das Projekt AGATA3S. *Deutsche Gesellschaft für Luft- und Raumfahrt, DLRK 27.-29.9.2022*. Dresden. doi:10.25967/570299
- Tapken, U., Meyer, R., Klähn, L., Behn (2024): Experimental investigation of the influence of boundary layer ingestion on the noise generation of a counter-rotating turbo fan, 30th AIAA/CEAS Aeroacoustics Conference, Rome, Italy, to be published
- Vinz, A., & Raichle, A. (2022). Investigation of the Effects of BLI Engine Integration on Aircraft Thrust Requirement. *Deutscher Luft- und Raumfahrtkongress 2022, 27.-29. Sept. 2022*. Dresden

Fan map



BLI impact on mean flow profile in fan inlet N=85, AL

plane E2a



plane E3

